9

MAGNETIZATION

9.0 INTRODUCTION

The sources of the magnetic fields considered in Chap. 8 were conduction currents associated with the motion of unpaired charge carriers through materials. Typically, the current was in a metal and the carriers were conduction electrons. In this chapter, we recognize that materials provide still other magnetic field sources. These account for the fields of permanent magnets and for the increase in inductance produced in a coil by insertion of a magnetizable material.

Magnetization effects are due to the propensity of the atomic constituents of matter to behave as magnetic dipoles. It is natural to think of electrons circulating around a nucleus as comprising a circulating current, and hence giving rise to a magnetic moment similar to that for a current loop, as discussed in Example 8.3.2.

More surprising is the magnetic dipole moment found for individual electrons. This moment, associated with the electronic property of *spin*, is defined as the *Bohr magneton*

$$m_e = \pm \frac{e}{m} \frac{1}{2} \hbar \tag{1}$$

where e/m is the electronic charge-to-mass ratio, 1.76×10^{11} coulomb/kg, and $2\pi\hbar$ is Planck's constant, $\hbar = 1.05 \times 10^{-34}$ joule-sec so that m_e has the units $A - m^2$. The quantum mechanics of atoms and molecules dictates that, whether due to the orbits or to the spins, the electronic contributions to their net dipole moments *tend* to cancel. Those that do make a contribution are typically in unfilled shells.

An estimate of the moment that would result if each atom or molecule of a material contributed only one Bohr magneton shows that the orbital and spin contributions from all the electrons comprising a typical solid had better tend to cancel or the resulting field effects would be prodigious indeed. Even if each atom or molecule is made to contribute only one Bohr magneton of magnetic moment, a

1

magnetic field results comparable to that produced by extremely large conduction currents. To make this apparent, compare the magnetic field induced by a current loop having a radius R and carrying a current i (Fig. 9.0.la) to that from a spherical collection of dipoles (Fig. 9.0.1b), each having the magnetic moment of only one electron.
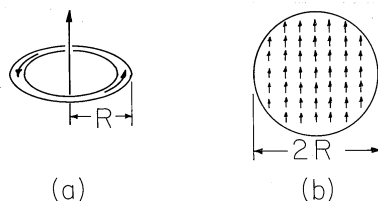

Fig. 9.0.1   (a) Current i in loop of radius R gives dipole moment **m**. (b) Spherical material of radius R has dipole moment approximated as the sum of atomic dipole moments.

In the case of the spherical material, we consider the net dipole moment to be simply the moment m_e of a single molecule multiplied by the number of molecules. The number of molecules per unit mass is Avogadro's number ($A_0 = 6.023 \times 10^{26}$ molecules/kg-mole) divided by the molecular weight, M_o. The mass is the volume multiplied by the mass density ρ (kg/m^3). Thus, for a sphere having radius R, the sum of the dipole moments is

$$m = m_e \Big(\frac{4}{3}\pi R^3 \rho\Big)\Big(\frac{A_o}{M_o}\Big) \tag{2}$$

Suppose that the current loop shown in Fig. 9.0.1a has the same radius R as the sphere. What current i would give rise to a magnetic moment equal to that from the sphere of hypothetical material? If the moment of the loop, given by (8.3.19) as being $m = i\pi R^2$, is set equal to that of the sphere, (2), it follows that i must be

$$i = m_e \frac{4}{3} R\rho \frac{A_o}{M_o} \tag{3}$$

Hence, for iron (where $\rho = 7.86 \times 10^3$ and $M_o = 56$) and a radius of 10 cm, the current required to produce the same magnetic moment is $10^5 A$.

Material magnetization can either be permanent or be induced by the application of a field, much as for the polarizable materials considered in Chap. 6. In most materials, the average moment per molecule that can be brought into play is much less than one Bohr magneton. However, highly magnetizable materials can produce net magnetic moments comparable to that estimated in (2).

The development of magnetization in this chapter parallels that for polarization in Chap. 6. Just as the polarization density was used in Sec. 6.1 to represent the effect of electric dipoles on the electric field intensity, the magnetization density introduced in Sec. 9.1 will account for the contributions of magnetic dipoles to the magnetic field intensity. The MQS laws and continuity conditions then collected in Sec. 9.2 are the basis for the remaining sections, and for Chap. 10 as well.

Because permanent magnets are so common, the permanent magnetization fields considered in Sec. 9.3 are more familiar than the permanent polarization electric fields of Sec. 6.3. Similarly, the force experienced as a piece of iron is brought

into a magnetic field is common evidence of the induced magnetization described by the constitutive laws of Sec. 9.4.

The extensive analogy between polarization and magnetization makes most of the examples from Chap. 6 analogous to magnetization examples. This is especially true in Secs. 9.5 and 9.6, where materials are considered that have a magnetization that is linearly related to the magnetic field intensity. Thus, these sections not only build on the insights gained in the earlier sections on polarization, but give the opportunity to expand on both topics as well. The magnetic circuits considered in Sec. 9.7 are of great practical interest and exemplify an approximate way for the evaluation of fields in the presence of strongly magnetized materials. The saturation of magnetizable materials is of primary practical concern. The problems for Secs. 9.6 and 9.7 are an introduction to fields in materials that are magnetically nonlinear.

We generalize Faraday's law in Sec. 9.2 so that it can be used in this chapter to predict the voltage at the terminals of coils in systems that include magnetization. This generalization is used to determine terminal relations that include magnetization in Sec. 9.5. The examples in the subsequent sections study the implications of Faraday's law with magnetization included. As in Chap. 8, we confine ourselves in this chapter to examples that can be modeled using the terminal variables of perfectly conducting circuits. The MQS laws, generalized in Sec. 9.2 to include magnetization, form the basis for the discussion of electric fields in MQS systems that is the theme of Chap. 10.

9.1 MAGNETIZATION DENSITY

The sources of magnetic field in matter are the (more or less) aligned magnetic dipoles of individual electrons or currents caused by circulating electrons.[1] We now describe the effect on the magnetic field of a distribution of magnetic dipoles representing the material.

In Sec. 8.3, we defined the magnitude of the magnetic moment m of a circulating current loop of current i and area a as $m = ia$. The moment vector, $\mathbf{m}$, was defined as normal to the surface spanning the contour of the loop and pointing in the direction determined by the right-hand rule. In Sec. 8.3, where the moment was in the z direction in spherical coordinates, the loop was found to produce the magnetic field intensity

$$\mathbf{H} = \frac{\mu_o m}{4\pi \mu_o r^3}[2\cos\theta \mathbf{i_r} + \sin\theta \mathbf{i_\theta}] \tag{1}$$

This field is analogous to the electric field associated with a dipole having the moment $\mathbf{p}$. With $\mathbf{p}$ directed along the z axis, the electric dipole field is given by taking the gradient of (4.4.10).

$$\mathbf{E} = \frac{p}{4\pi \epsilon_o r^3}[2\cos\theta \mathbf{i_r} + \sin\theta \mathbf{i_\theta}] \tag{2}$$

---

[1] Magnetic monopoles, which would play a role with respect to magnetic fields analogous to that of the charge with respect to electric fields, may in fact exist, but are certainly not of engineering significance. See *Science*, Research News, "In search of magnetic monopoles," Vol. 216, p. 1086 (June 4, 1982).

Thus, the dipole fields are obtained from each other by making the identifications

$$\boxed{\mathbf{p} \leftrightarrow \mu_o \mathbf{m}} \tag{3}$$

In Sec. 6.1, a spatial distribution of electric dipoles is represented by the polarization density $\mathbf{P} = N\mathbf{p}$, where N is the number density of dipoles. Similarly, here we define a *magnetization density* as

$$\boxed{\mathbf{M} = N\mathbf{m}} \tag{4}$$

where again N is the number of dipoles per unit volume. Note that just as the analog of the dipole moment $\mathbf{p}$ is $\mu_o \mathbf{m}$, the analog of the polarization density $\mathbf{P}$ is $\mu_o \mathbf{M}$.

9.2 LAWS AND CONTINUITY CONDITIONS WITH MAGNETIZATION

Recall that the effect of a spatial distribution of electric dipoles upon the electric field is described by a generalization of Gauss' law for electric fields, (6.2.1) and (6.2.2),

$$\nabla \cdot \epsilon_o \mathbf{E} = -\nabla \cdot \mathbf{P} + \rho_u \tag{1}$$

The effect of the spatial distribution of magnetic dipoles upon the magnetic field intensity is now similarly taken into account by generalizing the magnetic flux continuity law.

$$\boxed{\nabla \cdot \mu_o \mathbf{H} = -\nabla \cdot \mu_o \mathbf{M}} \tag{2}$$

In this law, there is no analog to an unpaired electric charge density.

The continuity condition found by integrating (2) over an incremental volume enclosing a section of an interface having a normal $\mathbf{n}$ is

$$\boxed{\mathbf{n} \cdot \mu_o(\mathbf{H}^a - \mathbf{H}^b) = -\mathbf{n} \cdot \mu_o(\mathbf{M}^a - \mathbf{M}^b)} \tag{3}$$

Suggested by the analogy to the description of polarization is the definition of the quantities on the right in (2) and (3), respectively, as the *magnetic charge density* ρ_m and the *magnetic surface charge density* σ_{sm}.

$$\boxed{\rho_m \equiv -\nabla \cdot \mu_o \mathbf{M}} \tag{4}$$

$$\boxed{\sigma_{sm} \equiv -\mathbf{n} \cdot \mu_o(\mathbf{M}^a - \mathbf{M}^b)} \tag{5}$$

Faraday's Law Including Magnetization.   The modification of the magnetic flux continuity law implies that another of Maxwell's equations must be generalized. In introducing the flux continuity law in Sec. 1.7, we observed that it was almost inherent in Faraday's law. Because the divergence of the curl is zero, the divergence of the *free space* form of Faraday's law reduces to

$$\nabla \cdot (\nabla \times \mathbf{E}) = 0 = -\frac{\partial}{\partial t}\nabla \cdot \mu_o \mathbf{H} \tag{6}$$

Thus, in free space, $\mu_o \mathbf{H}$ must have a divergence that is at least constant in time. The magnetic flux continuity law adds the information that this constant is zero. In the presence of magnetizable material, (2) shows that the quantity $\mu_o(\mathbf{H} + \mathbf{M})$ is solenoidal. To make Faraday's law consistent with this requirement, the law is now written as

$$\boxed{\nabla \times \mathbf{E} = -\frac{\partial}{\partial t}\mu_o(\mathbf{H} + \mathbf{M})} \tag{7}$$

Magnetic Flux Density.   The grouping of $\mathbf{H}$ and $\mathbf{M}$ in Faraday's law and the flux continuity law makes it natural to *define* a new variable, the *magnetic flux density* $\mathbf{B}$.

$$\boxed{\mathbf{B} \equiv \mu_o(\mathbf{H} + \mathbf{M})} \tag{8}$$

This quantity plays a role that is analogous to that of the electric displacement flux density $\mathbf{D}$ defined by (6.2.14). Because there are no macroscopic quantities of monopoles of magnetic charge, its divergence is zero. That is, the flux continuity law, (2), becomes simply

$$\boxed{\nabla \cdot \mathbf{B} = 0} \tag{9}$$

and the corresponding continuity condition, (3), becomes simply

$$\boxed{\mathbf{n} \cdot (\mathbf{B}^a - \mathbf{B}^b) = 0} \tag{10}$$

A similar simplification is obtained by writing Faraday's law in terms of the magnetic flux density. Equation (7) becomes

$$\boxed{\nabla \times \mathbf{E} = -\frac{\partial \mathbf{B}}{\partial t}} \tag{11}$$

If the magnetization is specified independent of $\mathbf{H}$, it is usually best to have it entered explicitly in the formulation by not introducing $\mathbf{B}$. However, if $\mathbf{M}$ is given

as a function of $\mathbf{H}$, especially if it is linear in $\mathbf{H}$, it is most convenient to remove $\mathbf{M}$ from the formulation by using $\mathbf{B}$ as a variable.

Terminal Voltage with Magnetization. In Sec. 8.4, where we discussed the terminal voltage of a perfectly conducting coil, there was no magnetization. The generalization of Faraday's law to include magnetization requires a generalization of the terminal relation.

The starting point in deriving the terminal relation was Faraday's integral law, (8.4.9). This law is generalized to included magnetization effects by replacing $\mu_o\mathbf{H}$ with $\mathbf{B}$. Otherwise, the derivation of the terminal relation, (8.4.11), is the same as before. Thus, the terminal voltage is again

$$\boxed{v = \frac{d\lambda}{dt}} \tag{12}$$

but now the flux linkage is

$$\boxed{\lambda \equiv \int_S \mathbf{B} \cdot d\mathbf{a}} \tag{13}$$

In Sec. 9.4 we will see that Faraday's law of induction, as reflected in these last two relations, is the basis for measuring $\mathbf{B}$.

9.3 PERMANENT MAGNETIZATION

As the modern-day versions of the lodestone, which made the existence of magnetic fields apparent in ancient times, permanent magnets are now so cheaply manufactured that they are used at home to pin notes on the refrigerator and so reliable that they are at the heart of motors, transducers, and information storage systems. To a first approximation, a permanent magnet can be modeled by a material having a specified distribution of magnetization density $\mathbf{M}$. Thus, in this section we consider the magnetic field intensity generated by prescribed distributions of $\mathbf{M}$.

In a region where there is no current density $\mathbf{J}$, Ampère's law requires that $\mathbf{H}$ be irrotational. It is then often convenient to represent the magnetic field intensity in terms of the scalar magnetic potential Ψ introduced in Sec. 8.3.

$$\mathbf{H} = -\nabla\Psi \tag{1}$$

From the flux continuity law, (9.2.2), it then follows that Ψ satisfies Poisson's equation.

$$\nabla^2\Psi = -\frac{\rho_m}{\mu_o}; \quad \rho_m \equiv -\nabla \cdot \mu_o\mathbf{M} \tag{2}$$

A specified magnetization density leads to a prescribed magnetic charge density ρ_m. The situation is analogous to that considered in Sec. 6.3, where the polarization density was prescribed and, as a result, where ρ_p was known.
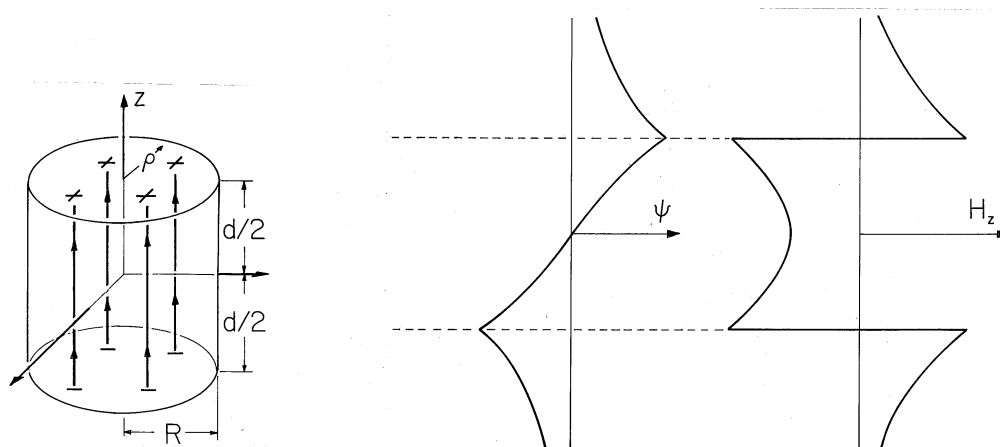
Fig. 9.3.1 (a) Cylinder of circular cross-section uniformly magnetized in the direction of its axis. (b) Axial distribution of scalar magnetic potential and (c) axial magnetic field intensity. For these distributions, the cylinder length is assumed to be equal to its diameter.

Of course, the net magnetic charge of a magnetizable body is always zero, because

$$\int_V \rho_m dv = \oint_S \mu_o \mathbf{H} \cdot d\mathbf{a} = 0 \tag{3}$$

if the integral is taken over the entire volume containing the body. Techniques for solving Poisson's equation for a prescribed charge distribution developed in Chaps. 4 and 5 are directly applicable here. For example, if the magnetization is given throughout all space and there are no other sources, the magnetic scalar potential is given by a superposition integral. Just as the integral of (4.2.2) is (4.5.3), so the integral of (2) is

$$\Psi = \int_{V'} \frac{\rho_m(\mathbf{r}')dv}{4\pi\mu_o|\mathbf{r} - \mathbf{r}'|} \tag{4}$$

If the region of interest is bounded by material on which boundary conditions are specified, (4) provides the particular solution.

Example 9.3.1.   Magnetic Field Intensity of a Uniformly Magnetized Cylinder

The cylinder shown in Fig. 9.3.1 is uniformly magnetized in the z direction, $\mathbf{M} = M_o \mathbf{i_z}$. The first step toward finding the resulting $\mathbf{H}$ within the cylinder and in the surrounding free space is an evaluation of the distribution of magnetic charge density. The uniform $\mathbf{M}$ has no divergence, so $\rho_m = 0$ throughout the volume. Thus, the source of $\mathbf{H}$ is on the surfaces where $\mathbf{M}$ originates and terminates. In view of (9.2.3), it takes the form of the surface charge density

$$\sigma_{sm} = -\mathbf{n} \cdot \mu_o(\mathbf{M}^a - \mathbf{M}_b) = \pm\mu_o M_o \tag{5}$$

The upper and lower signs refer to the upper and lower surfaces.

In principle, we could use the superposition integral to find the potential everywhere. To keep the integration simple, we confine ourselves here to finding it on the z axis. The integration of (4) then reduces to integrations over the endfaces of the cylinder.

$$\Psi = \int_0^R \frac{\mu_o M_o 2\pi \rho' d\rho'}{4\pi\mu_o \sqrt{\rho'^2 + \left(z - \frac{d}{2}\right)^2}} - \int_0^R \frac{\mu_o M_o 2\pi \rho' d\rho'}{4\pi\mu_o \sqrt{\rho'^2 + \left(z + \frac{d}{2}\right)^2}} \tag{6}$$

With absolute magnitudes used to make the expressions valid regardless of position along the z axis, these integrals become

$$\begin{aligned}
\Psi = \frac{dM_o}{2}\Bigg[&\sqrt{\left(\frac{R}{d}\right)^2 + \left(\frac{z}{d} - \frac{1}{2}\right)^2} - \left|\frac{z}{d} - \frac{1}{2}\right| \\
&- \sqrt{\left(\frac{R}{d}\right)^2 + \left(\frac{z}{d} + \frac{1}{2}\right)^2} + \left|\frac{z}{d} + \frac{1}{2}\right|\Bigg]
\end{aligned} \tag{7}$$

The field intensity follows from (1)

$$H_z = -\frac{dM_o}{2}\left[\frac{\left(\frac{z}{d} - \frac{1}{2}\right)}{\sqrt{\left(\frac{R}{d}\right)^2 + \left(\frac{z}{d} - \frac{1}{2}\right)^2}} - \frac{\left(\frac{z}{d} + \frac{1}{2}\right)}{\sqrt{\left(\frac{R}{d}\right)^2 + \left(\frac{z}{d} + \frac{1}{2}\right)^2}} + u\right] \tag{8}$$

where $u \equiv 0$ for $|z| > d/2$ and $u \equiv 2$ for $-d/2 < z < d/2$. Here, from top to bottom, respectively, the signs correspond to evaluating the field above the upper surface, within the magnet, and below the bottom surface.

The axial distributions of Ψ and H_z shown in Fig. 9.3.1 are consistent with a three-dimensional picture of a field that originates on the top face of the magnet and terminates on the bottom face. As for the spherical magnet (the analogue of the permanently polarized sphere shown in Fig. 6.3.1), the magnetic field intensity inside the magnet has a direction opposite to that of **M**.

In practice, **M** would most likely be determined by making measurements of the external field and then deducing **M** from this field.

If the magnetic field intensity is generated by a combination of prescribed currents and permanent magnetization, it can be evaluated by superimposing the field due to the current and the magnetization. For example, suppose that the uniformly magnetized circular cylinder of Fig. 9.3.1 were surrounded by the N-turn solenoid of Fig. 8.2.3. Then the axial field intensity would be the sum of that for the current [predicted by the Biot-Savart law, (8.2.7)], and for the magnetization [predicted by the negative gradient of (4)].

Example 9.3.2.   Retrieval of Signals Stored on Magnetizable Tape

Permanent magnetization is used for a permanent record in the tape recorder. Currents in an electromagnet are used to induce the permanent magnetization, exploiting the hysteresis in the magnetization of certain materials, as will be discussed
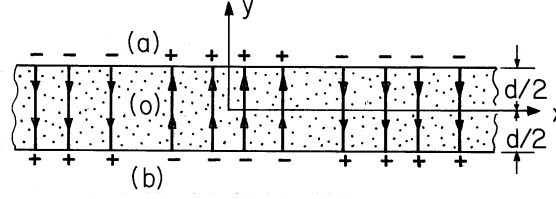
Fig. 9.3.2   Permanently magnetized tape has distribution of **M** representing a Fourier component of a recorded signal. From a frame of reference attached to the tape, the magnetization is static.
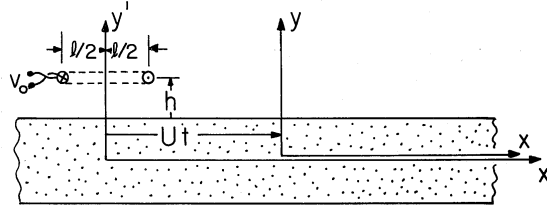

Fig. 9.3.3   From the frame of reference of a sensing coil, the tape is seen to move in the x' direction with the velocity U.

in Sec. 9.4. Here we look at a model of perpendicular magnetization, an actively pursued research field. The conventional recording is done by producing magnetization **M** parallel to the tape.

In a thin tape at rest, the magnetization density shown in Fig. 9.3.2 is assumed to be uniform over the thickness and to be of the simple form

$$\mathbf{M} = M_o \cos \beta x \mathbf{i_y} \tag{9}$$

The magnetic field is first determined in a frame of reference attached to the tape, denoted by (x, y, z) as defined in Fig. 9.3.2. The tape moves with a velocity U with respect to a fixed sensing "head," and so our second step will be to represent this field in terms of fixed coordinates. With Fig. 9.3.3 in view, it is clear that these coordinates, denoted by (x', y', z'), are related to the moving coordinates by

$$x' = x + Ut \rightarrow x = x' - Ut; \qquad y = y' \tag{10}$$

Thus, from the fixed reference frame, the magnetization takes the form of a traveling wave.

$$\mathbf{M} = M_o \cos \beta (x' - Ut) \mathbf{i_y} \tag{11}$$

If **M** is observed at a fixed location x', it has a sinusoidal temporal variation with the frequency $\omega = \beta U$. This relationship between the fixed frame frequency and the spatial periodicity suggests how the distribution of magnetization is established by "recording" a signal having the frequency ω.

The magnetization density has no divergence in the volume of the tape, so the field source is a surface charge density. With upper and lower signs denoting the upper and lower tape surfaces, it follows that

$$\sigma_m = \pm \mu_o M_o \cos \beta x \tag{12}$$

The continuity conditions to be satisfied at the upper and lower surfaces represent the continuity of magnetic flux (9.2.3)

$$\mu_o H_y^a - \mu_o H_y^o = \mu_o M_o \cos \beta x \quad \text{at} \quad y = \frac{d}{2}$$

$$\mu_o H_y^o - \mu_o H_y^b = -\mu_o M_o \cos \beta x \quad \text{at} \quad y = -\frac{d}{2} \tag{13}$$

and the continuity of tangential **H**

$$\Psi_a = \Psi_o \quad \text{at} \quad y = \frac{d}{2}$$

$$\Psi_o = \Psi_b \quad \text{at} \quad y = -\frac{d}{2} \tag{14}$$

In addition, the field should go to zero as $y \to \pm\infty$.

   Because the field sources are confined to surfaces, the magnetic scalar potential must satisfy Laplace's equation, (2) with $\rho_m = 0$, in the bulk regions delimited by the interfaces. Motivated by the "odd" symmetry of the source with respect to the $y = 0$ plane and its periodicity in x, we pick solutions to Laplace's equation for the magnetic potential above (a), inside (o), and below (b) the tape that also satisfy the odd symmetry condition of having $\Psi(y) = -\Psi(-y)$.

$$\psi_a = A\, e^{-\beta y} \cos \beta x$$

$$\psi_o = C\, \sinh \beta y \cos \beta x \tag{15}$$

$$\psi_b = -A\, e^{\beta y} \cos \beta x$$

Subject to the requirement that $\beta > 0$, the exterior potentials go to zero at $y = \pm\infty$. The interior function is made an odd function of y by excluding the $\cosh(\beta y)\cos(\beta x)$ solution to Laplace's equation, while the exterior functions are made odd by making the coefficients equal in magnitude and opposite in sign. Thus, only two coefficients remain to be determined. These follow from substituting the assumed solution into either of (13) and either of (14), and then solving the two equations to obtain

$$A = \frac{M_o}{\beta} e^{\beta d/2} \left(1 + \coth \frac{\beta d}{2}\right)^{-1}$$

$$C = \frac{M_o}{\beta} \left[\left(1 + \coth \frac{\beta d}{2}\right) \sinh \frac{\beta d}{2}\right]^{-1} \tag{16}$$

The conditions at one interface are automatically satisfied if those at the other are met. This is a proof that the assumed solutions have indeed been correct. Our foresight in defining the origin of the y axis to be at the symmetry plane and exploiting the resulting odd dependence of Ψ on y has reduced the number of undetermined coefficients from four to two.

   This field is now expressed in the fixed frame coordinates. With A defined by (16a) and x and y given in terms of the fixed frame coordinates by (10), the magnetic potential above the tape has been determined to be

$$\Psi_a = \frac{M_o}{\beta} \frac{e^{-\beta(y' - \frac{d}{2})}}{\left(1 + \coth \frac{\beta d}{2}\right)} \cos \beta(x' - Ut) \tag{17}$$

Next, we determine the output voltage of a fixed coil, positioned at a height h above the tape, as shown in Fig. 9.3.3. This detecting "head" has N turns, a length l in the x' direction, and width w in the z direction. With the objective of finding the flux linkage, we use (17) to determine the y-directed flux density in the neighborhood of the coil.

$$B_y = -\mu_o \frac{\partial \Psi_a}{\partial y'} = \frac{\mu_o M_o e^{-\beta(y' - \frac{d}{2})}}{\left(1 + \coth \frac{\beta d}{2}\right)} \cos \beta(x' - Ut) \tag{18}$$
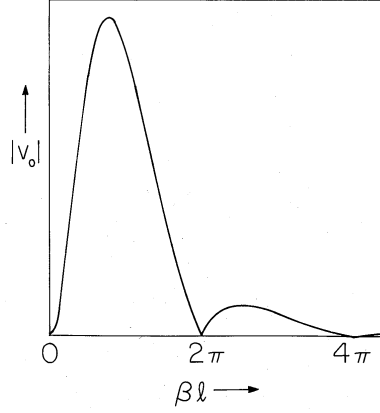
Fig. 9.3.4   Magnitude of sensing coil output voltage as a function of $\beta l = 2\pi l/\Lambda$, where Λ is the wavelength of the magnetization. If the magnetization is produced by a fixed coil driven at the angular frequency ω, the horizontal axis, which is then $\omega l/U$, is proportional to the recording frequency.

The flux linkage follows by multiplying the number of turns N times B_y integrated over the surface in the plane $y = h + \frac{1}{2}d$ spanned by the coil.

$$
\begin{aligned}
\lambda &= wN \int_{-l/2}^{l/2} B_y\left(y' = h + \frac{d}{2}\right) dx' \\
&= \frac{\mu_o M_o wN e^{-\beta h}}{\beta\left(1 + \coth\frac{\beta d}{2}\right)} \left[\sin\beta\left(\frac{l}{2} - Ut\right) + \sin\beta\left(\frac{l}{2} + Ut\right) \right]
\end{aligned}
\tag{19}
$$

The dependence on l is clarified by using a trigonometric identity to simplify the last term in this expression.

$$
\lambda = \frac{2\mu_o M_o wN e^{-\beta h}}{\beta\left(1 + \coth\frac{\beta d}{2}\right)} \sin\frac{\beta l}{2} \cos\beta Ut
\tag{20}
$$

Finally, the output voltage follows from (9.2.12).

$$
v_o = \frac{d\lambda}{dt} = -\frac{2\mu_o M_o wUN}{\left(1 + \coth\frac{\beta d}{2}\right)} e^{-\beta h} \sin\frac{\beta l}{2} \sin\beta Ut
\tag{21}
$$

The strong dependence of this expression on the wavelength of the magnetization, $2\pi/\beta$, reflects the nature of fields predicted using Laplace's equation. It follows from (21) that the output voltage has the angular frequency $\omega = \beta U$. Thus, (21) can also be regarded as giving the frequency response of the sensor. The magnitude of v_o has the dependence on either the normalized β or ω shown in Fig. 9.3.4.

Two phenomena underlie the voltage response. The periodic dependence reflects the relationship between the length l of the coil and the wavelength $2\pi/\beta$ of the magnetization. When the coil length is equal to the wavelength, there is as much positive as negative flux linking the coil at a given instant, and the signal falls to zero. This is also the condition when l is any multiple of a wavelength and accounts for the $\sin(\frac{1}{2}\beta l)$ term in (21).
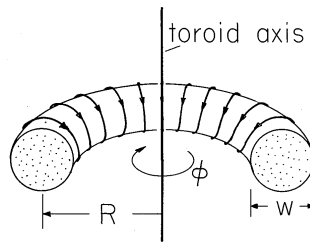
Fig. 9.4.1   Toroidal coil with donut-shaped magnetizable core.

The strong decay of the envelope of the output signal as the frequency is increased, and hence the wavelength decreased, reflects a property of Laplace's equation that frequently comes into play in engineering electromagnetic fields. The shorter the wavelength, the more rapid the decay of the field in the direction perpendicular to the tape. With the sensing coil at a fixed height above the tape, this means that once the wavelength is on the order of $2\pi h$, there is an essentially exponential decrease in signal with increasing frequency. Thus, there is a strong incentive to place the coil as close to the tape as possible.

We should expect that if the tape is very thin compared to the wavelength, the field induced by magnetic surface charges on the top surface would tend to be canceled by those of opposite sign on the surface just below. This effect is accounted for by the term $[1 + \coth(\frac{1}{2}\beta d)]$ in the denominator of (21).

In a practical recording device, the sensing head of the previous example would incorporate magnetizable materials. To predict how these affect the fields, we need a law relating the field to the magnetization it induces. This is the subject of the next section.

9.4 MAGNETIZATION CONSTITUTIVE LAWS

The permanent magnetization model of Sec. 9.3 is a somewhat artificial example of the magnetization density $\mathbf{M}$ specified, independent of the magnetic field intensity. Even in the best of permanent magnets, there is actually some dependence of $\mathbf{M}$ on $\mathbf{H}$.

Constitutive laws relate the magnetization density $\mathbf{M}$ or the magnetic flux density $\mathbf{B}$ to the macroscopic $\mathbf{H}$ within a material. Before discussing some of the more common relations and their underlying physics, it is well to have in view an experiment giving direct evidence of the constitutive law of magnetization. The objective is to observe the establishment of $\mathbf{H}$ by a current in accordance with Ampère's law, and deduce $\mathbf{B}$ from the voltage it induces in accordance with Faraday's law.

Example 9.4.1.   Toroidal Coil

A coil of toroidal geometry is shown in Fig. 9.4.1. It consists of a donut-shaped core filled with magnetizable material with N_1 turns tightly wound on its periphery. By means of a source driving its terminals, this coil carries a current i. The resulting
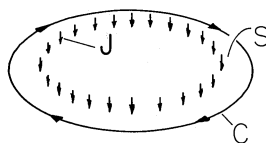
Fig. 9.4.2   Surface S enclosed by contour C used with Ampère's integral law to determine **H** in the coil shown in Fig. 9.4.1.

current distribution can be assumed to be so smooth that the fine structure of the field, caused by the finite size of the wires, can be disregarded. We will ignore the slight pitch of the coil and the associated small current component circulating around the axis of the toroid.

Because of the toroidal geometry, the H field in the magnetizable material is determined by Ampère's law and symmetry considerations. Symmetry about the toroidal axis suggests that **H** is ϕ directed. The integral MQS form of Ampère's law is written for a contour C circulating about the toroidal axis within the core and at a radius r. Because the major radius R of the torus is large compared to the minor radius $\frac{1}{2}w$, we will ignore the variation of r over the cross-section of the torus and approximate r by an average radius R. The surface S spanned by this contour and shown in Fig. 9.4.2 is pierced N_1 times by the current i, giving a total current of $N_1 i$. Thus, the azimuthal field inside the core is essentially

$$2\pi r H_\phi = N_1 i \rightarrow H_\phi \equiv H = \frac{N_1 i}{2\pi r} \simeq \frac{N_1 i}{2\pi R} \tag{1}$$

Note that the same argument shows that the magnetic field intensity outside the core is zero.

In general, if we are given the current distribution and wish to determine **H**, recourse must be made not only to Ampère's law but to the flux continuity condition as well. In the idealized toroidal geometry, where the flux lines automatically close on themselves without leaving the magnetized material, the flux continuity condition is automatically satisfied. Thus, in the toroidal configuration, the **H** imposed on the core is determined by a measurement of the current i and the geometry.

How can we measure the magnetic flux density in the core? Because **B** appears in Faraday's law of induction, the measurement of the terminal voltage of an additional coil, having N_2 turns also wound on the donut-shaped core, gives information on **B**. The terminals of this coil are terminated in a high enough impedance so that there is a negligible current in this second winding. Thus, the **H** field established by the current i remains unaltered.

The flux linked by each turn of the sensing coil is essentially the flux density multiplied by the cross-sectional area $\pi w^2/4$ of the core. Thus, the flux linked by the terminals of the sensing coil is

$$\lambda_2 = \frac{\pi w^2}{4} N_2 B \tag{2}$$

and flux density in the core material is directly reflected in the terminal flux-linkage.

The following demonstration shows how (1) and (2) can be used to infer the magnetization characteristic of the core material from measurement of the terminal current and voltage of the first and second coils.

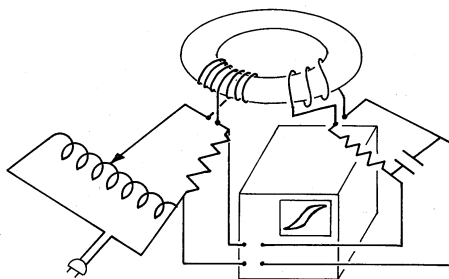**Demonstration 9.4.1.   Measurement of $B - H$ Characteristic**

Fig. 9.4.3 Demonstration in which the $B - H$ curve is traced out in the sinusoidal steady state.

The experiment shown in Fig. 9.4.3 displays the magnetization characteristic on the oscilloscope. The magnetizable material is in the donut-shaped toroidal configuration of Example 9.4.1 with the N_1-turn coil driven by a current i from a Variac. The voltage across a series resistance then gives a horizontal deflection of the oscilloscope proportional to H, in accordance with (1).

The terminals of the N_2 turn-coil are connected through an integrating network to the vertical deflection terminals of the oscilloscope. Thus, the vertical deflection is proportional to the integral of the terminal voltage, to λ, and hence through (2), to **B**.

In the discussions of magnetization characteristics which follow, it is helpful to think of the material as comprising the core of the torus in this experiment. Then the magnetic field intensity **H** is proportional to the current i, while the magnetic flux density **B** is reflected in the voltage induced in a coil linking this flux.

Many materials are *magnetically linear* in the sense that

$$\boxed{\mathbf{M} = \chi_m \mathbf{H}} \tag{3}$$

Here χ_m is the *magnetic susceptibility.* More commonly, the constitutive law for a magnetically linear material is written in terms of the magnetic flux density, defined by (9.2.8).

$$\boxed{\mathbf{B} = \mu \mathbf{H}; \qquad \mu \equiv \mu_o(1 + \chi_m)} \tag{4}$$

According to this law, the magnetization is taken into account by replacing the permeability of free space μ_o by the *permeability* μ of the material. For purposes of comparing the magnetizability of materials, the *relative permeability* μ/μ_o is often used.

Typical susceptibilities for certain elements, compounds, and common materials are given in Table 9.4.1. Most common materials are only slightly magnetizable. Some substances that are readily polarized, such as water, are not easily magnetized. Note that the magnetic susceptibility can be either positive or negative and that there are some materials, notably iron and its compounds, in which it can be enormous. In establishing an appreciation for the degree of magnetizability that can be expected of a material, it is helpful to have a qualitative picture of its mi-

TABLE 9.4.1 RELATIVE SUSCEPTIBILITIES OF COMMON MATERIALS		
	Material	χ_m
PARAMAGNETIC	Mg	1.2×10^{-5}
	Al	2.2×10^{-5}
	Pt	3.6×10^{-4}
	air	3.6×10^{-7}
	O_2	2.1×10^{-6}
DIAMAGNETIC	Na	-0.24×10^{-5}
	Cu	-1.0×10^{-5}
	diamond	-2.2×10^{-5}
	Hg	-3.2×10^{-5}
	H_2O	-0.9×10^{-5}
FERROMAGNETIC	Fe (dynamo sheets)	5.5×10^3
	Fe (lab specimens)	8.8×10^4
	Fe (crystals)	1.4×10^6
	Si-Fe transformer sheets	7×10^4
	Si-Fe crystals	3.8×10^6
	μ-metal	10^5
FERRIMAGNETIC	Fe_3O_4	100
	ferrites	5000

croscopic origins, beginning at the atomic level but including the collective effects of groups of atoms or molecules that result when they become as densely packed as they are in solids. These latter effects are prominent in the most easily magnetized materials.

The magnetic moment of an atom (or molecule) is the sum of the orbital and spin contributions. Especially in a gas, where the atoms are dilute, the magnetic susceptibility results from the (partial) alignment of the individual magnetic moments by a magnetic field. Although the spin contributions to the moment tend to cancel, many atoms have net moments of one or more Bohr magnetons. At room temperature, the orientations of the moments are mostly randomized by thermal agitation, even under the most intense fields. As a result, an applied field can give rise to a significant magnetization only at very low temperatures. A *paramagnetic material* displays an appreciable susceptibility only at low temperatures.

If, in the absence of an applied field, the spin contributions to the moment of an atom very nearly cancel, the material can be *diamagnetic*, in the sense that it displays a slightly negative susceptibility. With the application of a field, the
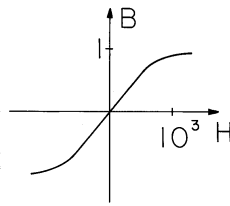
Fig. 9.4.4   Typical magnetization curve without hysteresis. For typical fer-romagnetic solids, the saturation flux density is in the range of 1–2 Tesla. For ferromagnetic domains suspended in a liquid, it is .02–.04 Tesla.

orbiting electrons are slightly altered in their circulations, giving rise to changes in moment in a direction opposite to that of the applied field. Again, thermal energy tends to disorient these moments. At room temperature, this effect is even smaller than that for paramagnetic materials.

At very low temperatures, it is possible to raise the applied field to such a level that essentially all the moments are aligned. This is reflected in the saturation of the flux density **B**, as shown in Fig. 9.4.4. At low field intensity, the slope of the magnetization curve is μ, while at high field strengths, there are no more moments to be aligned and the slope is μ_o. As long as the field is raised and lowered at a rate slow enough so that there is time for the thermal energy to reach an equilibrium with the magnetic field, the *B-H* curve is single valued in the sense that the same curve is followed whether the magnetic field is increasing or decreasing, and regardless of its rate of change.

Until now, we have been considering the magnetization of materials that are sufficiently dilute so that the atomic moments do not interact with each other. In solids, atoms can be so closely spaced that the magnetic field due to the moment of one atom can have a significant effect on the orientation of another. In *ferromagnetic* materials, this mutual interaction is all important.

To appreciate what makes certain materials ferromagnetic rather than simply paramagnetic, we need to remember that the electrons which surround the nuclei of atoms are assigned by quantum mechanical principles to layers or "shells." Each shell has a particular maximum number of electrons. The electron behaves as if it possessed a net angular momentum, or spin, and hence a magnetic moment. A filled shell always contains an even number of electrons which are distributed spatially in such a manner that the total spin, and likewise the magnetic moment, is zero.

For the majority of atoms, the outermost shell is unfilled, and so it is the outer-most electrons that play the major role in determining the net magnetic moment of the atom. This picture of the atom is consistent with paramagnetic and diamagnetic behavior. However, the transition elements form a special class. They have unfilled *inner* shells, so that the electrons responsible for the net moment of the atom are surrounded by the electrons that interact most intimately with the electrons of a neighboring atom. When such atoms are as closely packed as they are in solids, the combination of the interaction between magnetic moments and of electrostatic coupling results in the *spontaneous* alignment of dipoles, or *ferromagnetism*. The underlying interaction between atoms is both magnetic and electrostatic, and can be understood only by invoking quantum mechanical arguments.

In a ferromagnetic material, atoms naturally establish an array of moments that reinforce. Nevertheless, on a macroscopic scale, ferromagnetic materials are
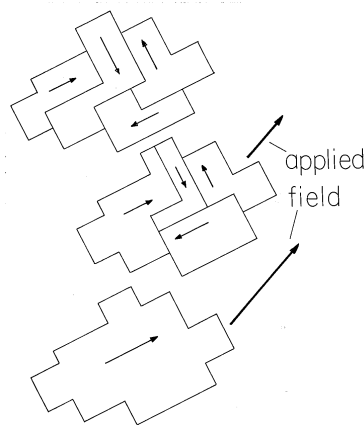
Fig. 9.4.5   Polycrystalline ferromagnetic material viewed at the domain level. In the absence of an applied magnetic field, the domain moments tend to cancel. (This presumes that the material has not been left in a magnetized state by a previously applied field.) As a field is applied, the domain walls shift, giving rise to a net magnetization. In ideal materials, saturation results as all of the domains combine into one. In materials used for bulk fabrication of transformers, imperfections prevent the realization of this state.

not necessarily permanently magnetized. The spontaneous alignment of dipoles is commonly confined to microscopic regions, called domains. The moments of the individual domains are randomly oriented and cancel on a macroscopic scale.

Macroscopic magnetization occurs when a field is applied to a solid, because those domains that have a magnetic dipole moment nearly aligned with the applied field grow at the expense of domains whose magnetic dipole moments are less aligned with the applied field. The shift in domain structure caused by raising the applied field from one level to another is illustrated in Fig. 9.4.5. The domain walls encounter a resistance to propagation that balances the effect of the field.

A typical trajectory traced out in the $B - H$ plane as the field is applied to a typical ferromagnetic material is shown in Fig. 9.4.6. If the magnetization is zero at the outset, the initial trajectory followed as the field is turned up starts at the origin. If the field is then turned down, the domains require a certain degree of coercion to reduce their average magnetization. In fact, with the applied field turned off, there generally remains a flux density, and the field must be reversed to reduce the flux density to zero. The trajectory traced out if the applied field is slowly cycled between positive and negative values many times is the one shown in the figure, with the *remanence flux density* $\mathbf{B}_r$ when $H = 0$ and a *coercive field intensity* $\mathbf{H}_c$ required to make the flux density zero. Some values of these parameters, for materials used to make permanent magnets, are given in Table 9.4.2.

In the toroidal geometry of Example 9.4.1, H is proportional to the terminal current i. Thus, imposition of a sinusoidally varying current results in a sinusoidally varying H, as illustrated in Fig. 9.4.6b. As the i and hence H increases, the trajectory in the $B - H$ plane is the one of increasing H. With decreasing H, a different trajectory is followed. In general, it is not possible to specify B simply by giving H (or even the time derivatives of H). When the magnetization state reflects the previous states of magnetization, the material is said to be *hysteretic*. The $B - H$

TABLE 9.4.2

**MAGNETIZATION PARAMETERS FOR
PERMANENT MAGNET**

From *American Institute of Physics Handbook,*
McGraw-Hill, p. 5–188.

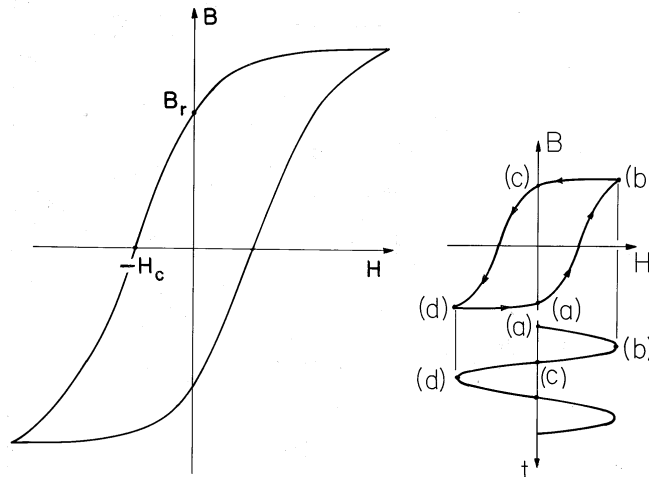| Material	H_c (A/m)	B_r (Tesla)
Carbon steel	4000	1.00
Alnico 2	43,000	0.72
Alnico 7	83,500	0.70
Ferroxdur 2	143,000	.34

Fig. 9.4.6   Magnetization characteristic for material showing hysteresis with
typical values of B_r and H_c given in Table 9.4.2. The curve is obtained after
many cycles of sinusoidal excitation in apparatus such as that of Fig. 9.4.3.
The trajectory is traced out in response to a sinusoidal current, as shown by
the inset.

trajectory representing the response to a sinusoidal H is then called the hysteresis
loop.

Hysteresis can be both harmful and useful. Permanent magnetization is one
result of hysteresis, and as we illustrated in Example 9.3.2, this can be the basis for
the storage of information on tapes. When we develop a picture of energy dissipation
in Chap. 11, it will be clear that hysteresis also implies the generation of heat, and
this can impose limits on the use of magnetizable materials.

Liquids having significant magnetizabilities have been synthesized by perma-
nently suspending macroscopic particles composed of single ferromagnetic domains.

Here also the relatively high magnetizability comes from the ferromagnetic character of the individual domains. However, the very different way in which the domains interact with each other helps in gaining an appreciation for the magnetization of ferromagnetic polycrystalline solids.

In the absence of a field imposed on the synthesized liquid, the thermal molecular energy randomizes the dipole moments and there is no residual magnetization. With the application of a low frequency H field, the suspended particles assume an average alignment with the field and a single-valued $B - H$ curve is traced out, typically as shown in Fig. 9.4.4. However, as the frequency is raised, the reorientation of the domains lags behind the applied field, and the $B - H$ curve shows hysteresis, much as for solids.

Although both the solid and the liquid can show hysteresis, the two differ in an important way. In the solid, the magnetization shows hysteresis even in the limit of zero frequency. In the liquid, hysteresis results only if there is a finite rate of change of the applied field.

Ferromagnetic materials such as iron are metallic solids and hence tend to be relatively good electrical conductors. As we will see in Chap. 10, this means that unless care is taken to interrupt conduction paths in the material, currents will be induced by a time-varying magnetic flux density. Often, these *eddy currents* are undesired. With the objective of obtaining a highly magnetizable insulating material, iron atoms can be combined into an oxide crystal. Although the spontaneous interaction between molecules that characterizes ferromagnetism is indeed observed, the alignment of neighbors is antiparallel rather than parallel. As a result, such pure oxides do not show strong magnetic properties. However, a mixed-oxide material like Fe_3O_4 (magnetite) is composed of sublattice oxides of differing moments. The spontaneous antiparallel alignment results in a net moment. The class of relatively magnetizable but electrically insulating materials are called *ferrimagnetic.*

Our discussion of the origins of magnetization began at the atomic level, where electronic orbits and spins are fundamental. However, it ends with a discussion of constitutive laws that can only be explained by bringing in additional effects that occur on scales much greater than atomic or molecular. Thus, the macroscopic **B** and **H** used to describe magnetizable materials can represent averages with respect to scales of domains or of macroscopic particles. In Sec. 9.5 we will make an artificial diamagnetic material from a matrix of "perfectly" conducting particles. In a time-varying magnetic field, a magnetic moment is induced in each particle that tends to cancel that being imposed, as was shown in Example 8.4.3. In fact, the currents induced in the particles and responsible for this induced moment are analogous to the induced changes in electronic orbits responsible on the atomic scale for diamagnetism[1].

9.5 FIELDS IN THE PRESENCE OF MAGNETICALLY
LINEAR INSULATING MATERIALS

In this and the next two sections, we study materials with the linear magnetization characteristic of (9.4.4). With the understanding that μ is a prescribed function of position, $\mathbf{B} = \mu\mathbf{H}$, the MQS forms of Ampère's law and the flux continuity law are

$$\boxed{\nabla \times \mathbf{H} = \mathbf{J}} \tag{1}$$

$$\boxed{\nabla \cdot \mu\mathbf{H} = 0} \tag{2}$$

In this chapter, we assume that the current density $\mathbf{J}$ is confined to perfect conductors. We will find in Chap. 10 that a time-varying magnetic flux implies an electric field. Thus, wherever a conducting material finds itself in a time-varying field, there is the possibility that *eddy currents* will be induced. It is for this reason that the magnetizable materials considered in this and the next sections are presumed to be insulating. If the fields of interest vary slowly enough, these induced currents can be negligible.

Ferromagnetic materials are often metallic, and hence also conductors. However, materials can be made both readily magnetizable and insulating by breaking up the conduction paths. By engineering at the molecular or domain scale, or even introducing laminations of magnetizable materials, the material is rendered essentially free of a current density $\mathbf{J}$. The considerations that determine the thickness of laminations used in transformers to prevent eddy currents will be taken up in Chap. 10.

In the regions outside the perfect conductors carrying the current $\mathbf{J}$ of (1), $\mathbf{H}$ is irrotational and $\mathbf{B}$ is solenoidal. Thus, we have a choice of representations. Either, as in Sec. 8.3, we can use the scalar magnetic potential and let $\mathbf{H} = -\nabla\Psi$, or we can follow the lead from Sec. 8.6 and use the vector potential to represent the flux density by letting $\mathbf{B} = \nabla \times \mathbf{A}$.

Where there are discontinuities in the permeability and/or thin coils modeled by surface currents, the continuity conditions associated with Ampère's law and the flux continuity law are used. With $\mathbf{B}$ expressed using the linear magnetization constitutive law, (1.4.16) and (9.2.10) become

$$\boxed{\mathbf{n} \times (\mathbf{H}^a - \mathbf{H}^b) = \mathbf{K}} \tag{3}$$

$$\boxed{\mathbf{n} \cdot (\mu_a\mathbf{H}^a - \mu_b\mathbf{H}^b) = 0} \tag{4}$$

The classification of physical configurations given in Sec. 6.5 for linearly polarizable materials is equally useful here. In the first of these, the region of interest is of uniform permeability. The laws summarized by (1) and (2) are the same as for free space except that μ_o is replaced by μ, so the results of Chap. 6 apply directly. Configurations made up of materials having essentially uniform permeabilities are of the greatest practical interest by far. Thus, piece-wise uniform systems are the theme of Secs. 9.6 and 9.7. The smoothly inhomogeneous systems that are the last category in Fig. 9.5.1 are of limited practical interest. However, it is sometimes useful, perhaps in numerical simulations, to regard the uniform and piece-wise uniform systems as special cases of the smoothly nonuniform systems.
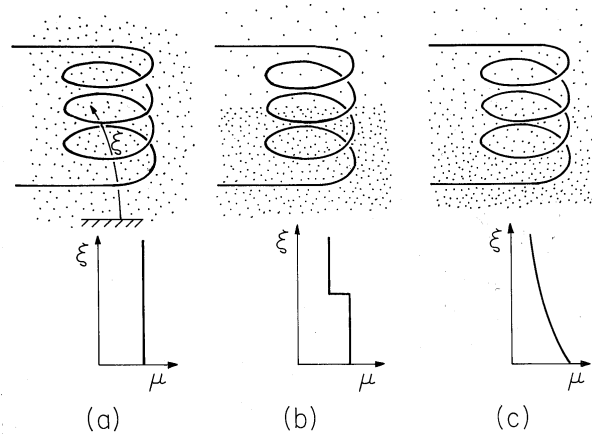
Fig. 9.5.1 (a) Uniform permeability, (b) piece-wise uniform permeability, and (c) smoothly inhomogeneous configurations involving linearly magnetizable material.

Inductance in the Presence of Linearly Magnetizable Materials.   In the presence of linearly magnetizable materials, the magnetic flux density is again proportional to the excitation currents. If fields are produced by a single perfectly conducting coil, its inductance is the generalization of that introduced with (8.4.13).

$$L \equiv \frac{\lambda}{i} = \frac{\int_S \mu \mathbf{H} \cdot d\mathbf{a}}{i} \tag{5}$$

The surface S spanning a contour defined by the perfectly conducting wire is the same as that shown in Figs. 8.4.3 and 8.4.4. The effect of having magnetizable material is, of course, represented in (5) by the effect of this material on the intensity, direction, and distribution of $\mathbf{B} = \mu \mathbf{H}$.

For systems in the first category of Fig. 9.5.1, where the entire region occupied by the field is filled by a material of uniform permeability μ, the effect of the magnetization on the inductance is clear. The solutions to (1) and (2) for $\mathbf{H}$ are not altered in the presence of the permeable material. It then follows from (5) that the inductance is simply proportional to μ.

Because it imposes a magnetic field intensity that never leaves the core material, the toroid of Example 9.4.1 is a special case of a piece-wise uniform magnetic material that acts as if all of space were filled with the magnetizable material. As shown by the following example, the inductance of the toroid is therefore also proportional to μ.

Example 9.5.1.   Inductance of a Toroid

If the toroidal core of the winding shown in Fig. 9.4.1 and used in the experiment of Fig. 9.4.3 were made a linearly magnetizable material, what would be the voltage needed to supply the driving current i? If we define the flux linkage of the driving coil as λ_1,
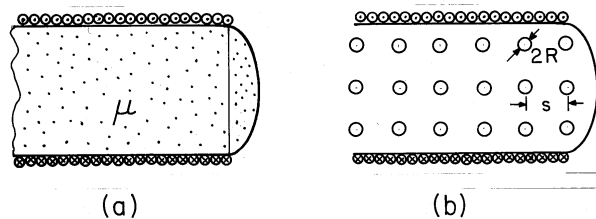
$$v = \frac{d\lambda_1}{dt} \tag{6}$$

Fig. 9.5.2   (a) Solenoid of length d and radius a filled with material of uniform permeability μ. (b) Solenoid of (a) filled with artificial diamagnetic material composed of an array of metal spheres having radius R and spacing s.

We now find the inductance L, where $\lambda_1 = Li$, and hence determine the required input voltage.

The flux linked by one turn of the driving coil is essentially the cross-sectional area of the toroid multiplied by the flux density. The total flux linked is this quantity multiplied by the total turns N_1.

$$\lambda_1 = N_1 \left(\frac{1}{4}\pi w^2 \right) B \tag{7}$$

According to the linear constitutive law, the flux density follows from the field intensity as $\mathbf{B} = \mu\mathbf{H}$. For the toroid, H is related to the driving current i by (9.4.1), so

$$B = \mu H = \mu \left(\frac{N_1}{2\pi R} \right) i \tag{8}$$

The desired relation is the combination of these last two expressions.

$$\lambda_1 = Li; \qquad L \equiv \frac{1}{8}\mu\frac{w^2}{R}N_1^2 \tag{9}$$

As predicted, the inductance is proportional to μ. Although inductances are generally increased by bringing paramagnetic and especially ferromagnetic materials into their fields, the effect of introducing ferromagnetic materials into coils can be less dramatic than in the toroidal geometry for reasons discussed in Sec. 9.6. The dependence of the inductance on the square of the turns results because not only is the field induced by the current i proportional to the number of turns, but so too is the amount of the resulting flux that is linked by the coil.

Example 9.5.2.   An Artificial Diamagnetic Material

The cross-section of a long (ideally "infinite") solenoid filled with material of uniform permeability is shown in Fig. 9.5.2a. The azimuthal surface current K_ϕ results in an axial magnetic field intensity $H_z = K_\phi$. We presume that the axial length d is very large compared to the radius a of the coil. Thus, the field inside the coil is uniform while that outside is zero. To see that this simple field solution is indeed correct, note that it is both irrotational and solenoidal everywhere except at the surface $r = a$, and that there the boundary conditions, (3) and (4), are satisfied.

For an n-turn coil carrying a current i, the surface current density $K_\phi = ni/d$. Thus, the magnetic field intensity is related to the terminal current by
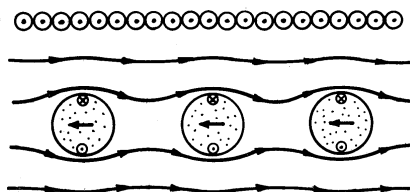
$$H_z = \frac{ni}{d} \tag{10}$$

Fig. 9.5.3   Inductance of the coil in Fig. 9.5.2b is decreased because perfectly conducting spheres tend to reduce its effective cross-sectional area.

In the linearly magnetized core region, the flux density is $B_z = \mu H_z$, and so it is also uniform. As a result, the flux linked by each turn is simply $\pi a^2 B_z$ and the total flux linked by the coil is

$$\lambda = n\pi a^2 \mu H_z \tag{11}$$

Substitution from (1) then gives

$$\lambda = Li, \qquad L \equiv \frac{\pi \mu a^2 n^2}{d} \tag{12}$$

where L is the inductance of the coil. Because the coil is assumed to be very long, its inductance is increased by a factor μ/μ_o over that of a coil in free space, much as for the toroid of Example 9.5.1.

Now suppose that the permeable material is actually a cubic array of metal spheres, each having a radius R, as shown in Fig. 9.5.2b. The frequency of the current i is presumably high enough so that each sphere can be regarded as perfectly conducting in the MQS sense discussed in Sec. 8.4. The spacing s of the spheres is large compared to their radius, so that the field of one sphere does not produce an appreciable field at the positions of its neighbors. Each sphere finds itself in an essentially uniform magnetic field.

The dipole moment of the currents induced in a sphere by a magnetic field that is uniform at infinity was calculated in Example 8.4.3, (8.4.21).

$$m = -2\pi H_o R^3 \tag{13}$$

Because the induced currents must produce a field that bucks out the imposed field, a negative moment is induced by a positive field.

By definition, the magnetization density is the number of magnetic moments per unit volume. For a cubic array with spacing s between the sphere centers, the number per unit volume is s^{-3}. Thus, the magnetization density is simply

$$M = Nm = -2\pi H_o \left(\frac{R}{s}\right)^3 \tag{14}$$

Comparison of this expression to (9.4.3), which defines the susceptibility χ_m, shows that

$$\chi_m = -2\pi \left(\frac{R}{s}\right)^3 \tag{15}$$

As we might have expected from the antiparallel moment induced in a sphere by an imposed field, the susceptibility is negative. The permeability, related to χ_m by (9.4.4), is therefore less than 1.

$$\mu = \mu_o(1 + \chi_m) = \mu_o \left[1 - 2\pi \left(\frac{R}{s}\right)^3\right] \tag{16}$$

The perfectly conducting spheres effectively reduce the cross-sectional area of the flux, as suggested by Fig. 9.5.3, and hence reduce the inductance. With the introduction of the array of metal spheres, the inductance goes from a value given by (12) with $\mu = \mu_o$ to one with μ given by (16).
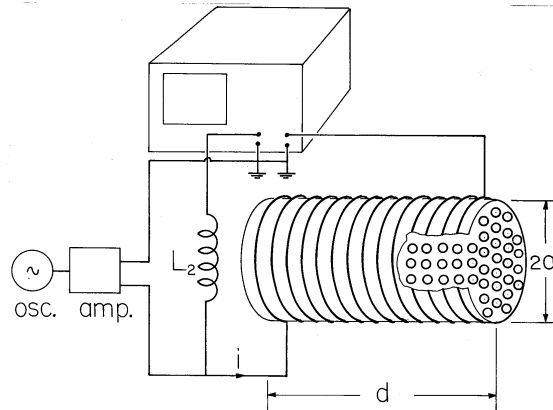
Fig. 9.5.4   Experiment to measure the decrease of inductance that results when the artificial diamagnetic array of Fig. 9.5.2b is inserted into a solenoid.

Faraday's law of induction is also responsible for diamagnetism due to atomic moments. Instead of inducing circulating conduction currents in a metal sphere, as in this example, the time-varying field induces changes in the orbits of electrons about the nucleus that, on the average, contribute an antiparallel magnetic moment to the atom.

The following demonstration is the MQS analog of the EQS Demonstration 6.6.1. In the latter, a measurement was made of the change in capacitance caused by inserting an artificial dielectric between capacitor plates. Here the change in inductance is observed as an artificial diamagnetic material is inserted into a solenoid. Although the spheres are modeled as perfectly conducting in both demonstrations, we will find in Chap. 10 that the requirements to justify this assumption in this MQS example are very different from those for its EQS counterpart.

Demonstration 9.5.1.   Artificial Diamagnetic Material

The experiment shown in Fig. 9.5.4 measures the change in solenoid inductance when an array of conducting spheres is inserted. The coil is driven at the angular frequency ω by an oscillator-amplifier. Over the length d shown in the figure, the field tends to be uniform. The circuit shown schematically in Fig. 9.5.5 takes the form of a bridge with the inductive reactance of L_2 used to balance the reactance of the central part of the empty solenoid.

The input resistances of the oscilloscope's balanced amplifiers, represented by R_s, are large compared to the inductor reactances. These branches dominate over the inductive reactances in determining the current through the inductors and, as a result, the inductor currents remain essentially constant as the inductances are varied. With the reactance of the inductor L_2 balancing that of the empty solenoid, these currents are equal and the balanced amplifier voltage $v_o = 0$. When the array of spheres is inserted into the solenoid, the currents through both legs remain essentially constant. Thus, the resulting voltage v_o is the change in voltage across the solenoid
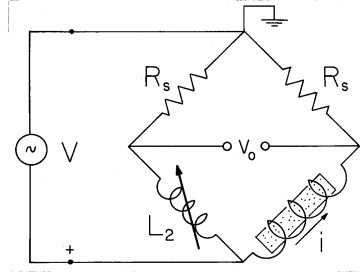
Fig. 9.5.5   Bridge used to measure the change in inductance in the experiment of Fig. 9.5.4.

caused by its change in inductance ΔL.

$$v_o = (\Delta L)\frac{di}{dt} \rightarrow |\hat{v}_o| = \omega(\Delta L)|\hat{i}| \tag{17}$$

In the latter expression, the current and voltage indicated by a circumflex are either peak or rms sinusoidal steady state amplitudes. In view of (12), this expression becomes

$$|\hat{v}_o| = \omega(\mu - \mu_o)\frac{\pi a^2 n^2}{d}|\hat{i}| \tag{18}$$

In terms of the sphere radius and spacing, the change in permeability is given by (16), so the voltage measured by the balanced amplifiers is

$$|\hat{v}_o| = \frac{2\pi^2 \omega a^2 n^2}{d}\left(\frac{R}{s}\right)^3|\hat{i}| \tag{19}$$

To evaluate this expression, we need only the frequency and amplitude of the coil current, the number of turns in the length d, and other dimensions of the system.

Induced Magnetic Charge: Demagnetization.   The complete analogy between linearly polarized and linearly magnetized materials is profitably carried yet another step. Magnetic charge is induced where μ is spatially varying, and hence the magnetizable material can introduce sources that revise the free space field distribution. In the linearly magnetizable material, the distribution of these sources is not known until after the fields have been determined. However, it is often helpful in qualitatively predicting the field effects of magnetizable materials to picture the distribution of induced magnetic charges.

Using a vector identity, (2) can be written

$$\mu \nabla \cdot \mathbf{H} + \mathbf{H} \cdot \nabla \mu = 0 \tag{20}$$

Rearrangement of this expression shows that the source of $\mu_o \mathbf{H}$, the magnetic charge density, is

$$\nabla \cdot \mu_o \mathbf{H} = -\frac{\mu_o}{\mu}\mathbf{H} \cdot \nabla \mu \equiv \rho_m \tag{21}$$

Most often we deal with piece-wise uniform systems where variations in μ are confined to interfaces. In that case, it is appropriate to write the continuity of flux density condition in the form

$$\mathbf{n} \cdot \mu_o(\mathbf{H}^a - \mathbf{H}^b) = \mathbf{n} \cdot \mu_o \mathbf{H}^a \big(1 - \frac{\mu_a}{\mu_b}\big) \equiv \sigma_{sm} \tag{22}$$

where σ_{sm} is the magnetic surface charge density. The following illustrates the use of this relation.

Illustration.   The Demagnetization Field

A sphere of material having uniform permeability μ is placed in an initially uniform upward-directed field. It is clear from (21) that there are no distortions of the uniform field from magnetic charge induced in the volume of the material. Rather, the sources of induced field are located on the surface where the imposed field has a component normal to the permeability discontinuity. It follows from (22) that positive and negative magnetic surface charges are induced on the top and bottom parts of the surface, respectively.

The $\mathbf{H}$ field caused by the induced magnetic surface charges originates at the positive charge at the top and terminates on the negative charge at the bottom. This is illustrated by the magnetization analog of the permanently polarized sphere, considered in Example 6.3.1. Our point here is that the field resulting from these induced magnetic surface charges tends to cancel the one imposed. Thus, the field intensity available to magnetize the material is reduced.

The remarks following (6.5.11) apply equally well here. The roles of $\mathbf{E}$, $\mathbf{D}$, and ϵ are taken by $\mathbf{H}$, $\mathbf{B}$, and μ. In regions of uniform permeability, (1) and (2) are the same laws considered in Chap. 8, and where the current density is zero, Laplace's equation governs. As we now consider piece-wise nonuniform systems, the effect of the material is accounted for by the continuity conditions.

9.6 FIELDS IN PIECE-WISE UNIFORM MAGNETICALLY LINEAR MATERIALS

Whether we choose to represent the magnetic field in terms of the magnetic scalar potential Ψ or the vector potential $\mathbf{A}$, in a current-free region having uniform permeability it assumes a distribution governed by Laplace's equation. That is, where μ is constant and $\mathbf{J} = 0$, (9.5.1) and (9.5.2) require that $\mathbf{H}$ is both solenoidal and irrotational. If we let $\mathbf{H} = -\nabla\Psi$, the field is automatically irrotational and

$$\boxed{\nabla^2\Psi = 0} \tag{1}$$

is the condition that it be solenoidal. If we let $\mu\mathbf{H} = \nabla \times \mathbf{A}$, the field is automatically solenoidal. The condition that it also be irrotational (together with the requirement that $\mathbf{A}$ be solenoidal) is then[2]

---

[2] $\nabla \times \nabla \times \mathbf{A} = \nabla(\nabla \cdot \mathbf{A}) - \nabla^2\mathbf{A}$

$$\boxed{\nabla^2 \mathbf{A} = 0} \tag{2}$$

Thus, in Cartesian coordinates, each component of $\mathbf{A}$ satisfies the same equation as does Ψ.

The methods illustrated for representing piece-wise uniform dielectrics in Sec. 6.6 are applicable here as well. The major difference is that here, currents are used to excite the field whereas there, unpaired charges were responsible for inducing the polarization. The sources are now the current density and surface current density rather than unpaired volume and surface charges. Thus, the external excitations drive the curl of the field, in accordance with (9.5.1) and (9.5.3), rather than its divergence.

The boundary conditions needed at interfaces between magnetically linear materials are

$$\boxed{\mathbf{n} \cdot (\mu_a \mathbf{H}^a - \mu_b \mathbf{H}^b) = 0} \tag{3}$$

for the normal component of the magnetic field intensity, and

$$\boxed{\mathbf{n} \times (\mathbf{H}^a - \mathbf{H}^b) = \mathbf{K}} \tag{4}$$

for the tangential component, in the presence of a surface current. As before, we shall find it convenient to represent windings by equivalent surface currents.

Example 9.6.1.   The Spherical Coil with a Permeable Core

The spherical coil developed in Example 8.5.1 is now filled with a uniform core having the permeability μ. With the field intensity again represented in terms of the magnetic scalar potential, $\mathbf{H} = -\nabla\Psi$, the analysis differs only slightly from that already carried out. Laplace's equation, (1), again prevails inside and outside the coil. At the coil surface, the tangential $\mathbf{H}$ again suffers a discontinuity equal to the surface current density in accordance with Ampère's continuity condition, (4). The effect of the permeable material is only felt through the flux continuity condition, (3), which requires that

$$\mu_o H_r^a - \mu H_r^b = 0 \tag{5}$$

Thus, the normal flux continuity condition of (8.5.12) is generalized to include the effect of the permeable material by

$$-\frac{\mu C}{R} = \frac{2\mu_o A}{R} \tag{6}$$

and it follows that the coefficients needed to evaluate Ψ, and hence $\mathbf{H}$, are now

$$A = \frac{Ni}{2\left(1 + \frac{2\mu_o}{\mu}\right)}; \qquad C = -\frac{\mu_o}{\mu}\frac{Ni}{\left(1 + \frac{2\mu_o}{\mu}\right)} \tag{7}$$

Substitution of these coefficients into (8.5.10) and (8.5.11) gives the field inside and outside the spherical coil.

$$\mathbf{H} = \begin{cases} \frac{\mu_o}{\mu} \frac{Ni}{\left(1 + \frac{2\mu_o}{\mu}\right)R}(\mathbf{i_r}\cos\theta - \mathbf{i}_\theta\sin\theta) = \frac{\mu_o}{\mu + 2\mu_o}\frac{Ni}{R}\mathbf{i_z}; & r < R \\ \frac{Ni}{2\left(1 + \frac{2\mu_o}{\mu}\right)R}\left(\frac{R}{r}\right)^3(\mathbf{i_r}2\cos\theta + \mathbf{i}_\theta\sin\theta); & r > R \end{cases} \tag{8}$$

If the coil is highly permeable, these expressions show that the field intensity inside is much less than that outside. In the limit of "infinite permeability," where $\mu_o/\mu \to 0$, the field inside is zero while that outside becomes

$$H_\theta(r = R) = \frac{Ni}{2R}\sin\theta \tag{9}$$

This is the surface current density, (8.5.6). *A surface current density backed by a highly permeable material terminates the tangential magnetic field.* Thus, Ampère's continuity condition relating the fields to each side of the surface is replaced by a boundary condition on the field on the low permeability side of the interface. Using this boundary condition, that H_θ^a be equal to the given K_θ, (8.5.6), the solution for the exterior Ψ and $\mathbf{H}$ can be written by inspection in the limit when $\mu \to \infty$.

$$\Psi_a = \frac{Ni}{2}\left(\frac{R}{r}\right)^2\cos\theta; \qquad \mathbf{H} = \frac{Ni}{2R}\left(\frac{R}{r}\right)^3(\mathbf{i_r}2\cos\theta + \mathbf{i}_\theta\sin\theta) \tag{10}$$

The interior magnetic flux density can in turn be *approximated* by using this exterior field to compute the flux density normal to the surface. Because this flux density must be the same inside, finding the interior field reduces to solving Laplace's equation for Ψ subject to the boundary condition that

$$-\mu\frac{\partial\Psi_b}{\partial r}(r = R) = \mu_o\frac{Ni}{R}\cos\theta \tag{11}$$

Again, the solution represents a uniform field and can be written by inspection.

$$\Psi_b = -\frac{\mu_o}{\mu}Ni\frac{r}{R}\cos\theta \tag{12}$$

The $\mathbf{H}$ field, the gradient of the above expression, is indeed that given by (8a) in the limit where μ_o/μ is small. Note that the interior $\mathbf{H}$ goes to zero as the permeability goes to infinity, but the interior flux density $\mathbf{B}$ remains finite. This fact makes it clear that the inductance of the coil must remain finite, even in the limit where $\mu \to \infty$.

To determine an expression for the inductance that is valid regardless of the core permeability, (8a) can be used to evaluate (8.5.18). Note that the internal flux density $\mathbf{B}$ that replaces $\mu_o H_z$ is $3\mu/[\mu + 2\mu_o]$ times larger than the flux density in the absence of the magnetic material. This enhancement factor increases monotonically with the ratio μ/μ_o but reaches a maximum of only 3 in the limit where this ratio goes to infinity. Once again, we have evidence of the core demagnetization caused by the surface magnetic charge induced on the surface of the sphere.

With the uniformity of the field inside the sphere known in advance, a much simpler derivation of (8a) gives further insight into the role of the magnetization.
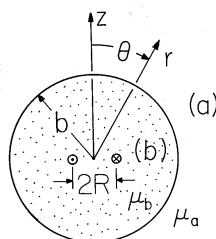
Fig. 9.6.1 Sphere of material having uniform permeability with N-turn coil of radius R at its center. Because $R \ll b$, the coil can be modeled as a dipole. The surrounding region has permeability μ_a.

Thus, in the core, the H-field is the superposition of two fields. The first is caused by the surface current, and given by (8a) with $\mu = \mu_o$.

$$H_i = \frac{Ni}{3R}\mathbf{i_z} \tag{13}$$

The second is due to the uniform magnetization $\mathbf{M} = M\mathbf{i_z}$, which is given by the magnetization analog to (6.3.15) ($\mathbf{E} \to \mathbf{H}$, $\mathbf{P} \to \mu_o\mathbf{M}$, $\epsilon_o \to \mu_o$).

$$\mathbf{H}_M = -\frac{M_o}{3}\mathbf{i_z} \tag{14}$$

The net internal magnetic field intensity is the sum of these.

$$\mathbf{H} = \Big(\frac{Ni}{3R} - \frac{M_o}{3}\Big)\mathbf{i_z} \tag{15}$$

Only now do we introduce the constitutive law relating M_o to H_z, $M_o = \chi_m H_z$. [In Sec. 9.8 we will exploit the fact that the relation could be nonlinear.] If this law is introduced into (15), and that expression solved for H_z, a result is obtained that is familiar from from (8a).

$$H_z = \frac{Ni/3R}{1 + \frac{1}{3}\chi_m} = \frac{\mu_o}{\mu}\frac{Ni/R}{\big(1 + \frac{2\mu_o}{\mu}\big)} \tag{16}$$

This last calculation again demonstrates how the field $Ni/3R$ is reduced by the magnetization through the "feedback factor" $1/[1 + (\chi_m/3)]$.

Magnetic circuit models, introduced in the next section, exploit the capacity of highly permeable materials to guide the magnetic flux. The example considered next uses familiar solutions to Laplace's equation to illustrate how this guiding takes place. We will make reference to this case study when the subject of magnetic circuits is initiated.

Example 9.6.2.   Field Model for a Magnetic Circuit

A small coil with N turns and excited by a current i is used to make a magnetic field in a spherically shaped material of permeability μ_b. As shown in Fig. 9.6.1, the coil has radius R, while the μ sphere has radius b and is surrounded by a magnetic medium of permeability μ_a.

Because the coil radius is small compared to that of the sphere, it will be modeled as a dipole having its moment $m = \pi R^2 i$ in the z direction. It follows from (8.3.13) that the magnetic scalar potential for this dipole is

$$\Psi_{\text{dipole}} = \frac{R^2 Ni}{4} \frac{\cos\theta}{r^2} \tag{17}$$

No surface current density exists at the surface of the sphere. Thus, Ampère's continuity law requires that

$$H_\theta^a - H_\theta^b = 0 \rightarrow \Psi_a = \Psi_b \quad \text{at} \quad r = b \tag{18}$$

Also, at the interface, the flux continuity condition is

$$\mu_a H_r^a - \mu_b H_r^b = 0 \quad \text{at} \quad r = b \tag{19}$$

Finally, the only excitation of the field is the coil at the origin, so we require that the field decay to zero far from the sphere.

$$\Psi_a \rightarrow 0 \quad \text{as} \quad r \rightarrow \infty \tag{20}$$

Given that the scalar potential has the θ dependence $\cos(\theta)$, we look for solutions having this same θ dependence. In the exterior region, the solution representing a uniform field is ruled out because there is no field at infinity. In the neighborhood of the origin, we know that Ψ must approach the dipole field. These two conditions are implicit in the assumed solutions

$$\Psi_a = A \frac{\cos\theta}{r^2}; \qquad \Psi_b = \frac{R^2 Ni}{4} \frac{\cos\theta}{r^2} + Cr\cos\theta \tag{21}$$

while the coefficients A and C are available to satisfy the two remaining continuity conditions, (18) and (19). Substitution gives two expressions which are linear in A and C and which can be solved to give

$$A = \frac{3}{4} \frac{\mu_b NiR^2}{(\mu_b + 2\mu_a)}; \qquad C = \frac{Ni}{b^3} \frac{R^2(\mu_b - \mu_a)}{2(\mu_b + 2\mu_a)} \tag{22}$$

We thus conclude that the scalar magnetic potential outside the sphere is that of a dipole

$$\Psi_a = \frac{3}{4} \frac{\mu_b Ni}{(\mu_b + 2\mu_a)} \left(\frac{R}{r}\right)^2 \cos\theta \tag{23}$$

while inside it is that of a dipole plus that of a uniform field.

$$\Psi_b = \frac{Ni}{4} \left[\left(\frac{R}{r}\right)^2 \cos\theta + \frac{2(\mu_b - \mu_a)}{(\mu_b + 2\mu_a)} \left(\frac{R}{b}\right)^2 \frac{r}{b} \cos\theta \right] \tag{24}$$

For increasing values of the relative permeability, the equipotentials and field lines are shown in Fig. 9.6.2. With $\mu_b/\mu_a = 1$, the field is simply that of the dipole at the origin. In the opposite extreme, where the ratio of permeabilities is 100, it has
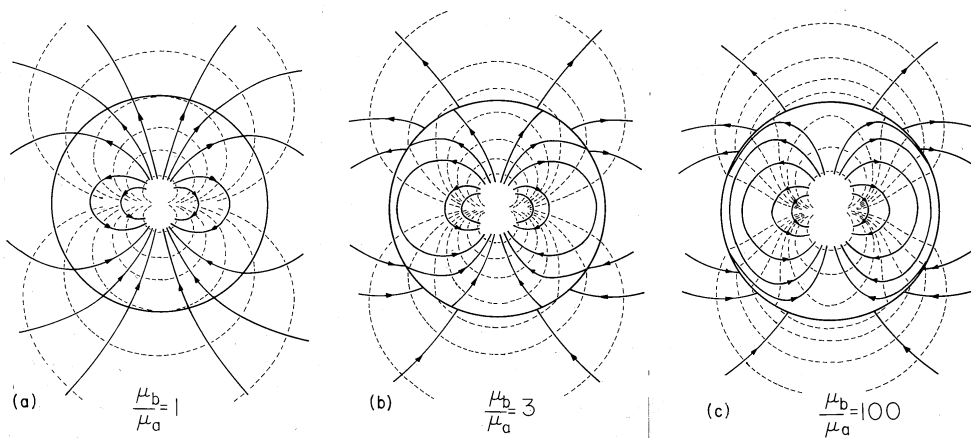
Fig. 9.6.2   Magnetic potential and lines of field intensity in and around the magnetizable sphere of Fig. 9.6.1. (a) With the ratio of permeabilities equal to 1, the dipole field extends into the surrounding free space region without modification. (b) With $\mu_b/\mu_a = 3$, field lines tend to be more confined to the sphere. (c) With $\mu_b/\mu_a = 100$, the field lines (and hence the flux lines) tend to remain inside the sphere.

become clear that the interior field lines tend to become tangential to the spherical surface.

The results of Fig. 9.6.2 can be elaborated by taking the limit of μ_b/μ_a going to infinity. In this limit, the scalar potentials are

$$\Psi_a = \frac{3}{4} Ni \left(\frac{R}{r}\right)^2 \cos\theta \tag{25}$$

$$\Psi_b = \frac{Ni}{r} \left(\frac{R}{b}\right)^2 \left[\left(\frac{b}{r}\right)^2 + 2\left(\frac{r}{b}\right)\right] \cos\theta \tag{26}$$

In the limit of a large permeability of the medium in which the coil is imbedded relative to that of the surrounding medium, guidance of the magnetic flux occurs by the highly permeable medium. Indeed, in this limit, the flux produced by the coil goes to infinity, whereas the flux of the field $\int \mathbf{H} \cdot d\mathbf{a}$ escaping from the sphere (the so-called "fringing") stays finite, because the exterior potential stays finite. The magnetic flux $\int \mathbf{B} \cdot d\mathbf{a}$ is guided within the sphere, and practically no magnetic flux escapes. The flux lines on the inside surface of the highly permeable sphere can be practically tangential as indeed predicted by (26).

Another limit of interest is when the outside medium is highly permeable and the coil is situated in a medium of low permeability (like free space). In this limit, one obtains

$$\Psi_a = 0 \tag{27}$$

$$\Psi_b = \frac{Ni}{4} \left(\frac{R}{b}\right)^2 \left[\left(\frac{b}{r}\right)^2 - \frac{r}{b}\right] \cos\theta \tag{28}$$

The surface at $r = b$ becomes an equipotential of Ψ. The magnetic field is perpendicular to the surface. The highly permeable medium behaves in a way analogous to a perfect conductor in the electroquasistatic case.
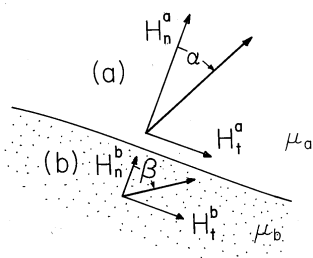
Fig. 9.6.3 Graphical representation of the relations between components of
H at an interface between a medium of permeability μ_a and a material having
permeability μ_b.

In order to gain physical insight, two types of approximate boundary conditions have been illustrated in the previous example. These apply when one region is of much greater permeability than another. In the limit of infinite permeability of one of the regions, the two continuity conditions at the interface between these regions reduce to one boundary condition on the fields in one of the regions. We conclude this section with a summary of these boundary conditions.

At a boundary between regions (a) and (b), having permeabilities μ_a and μ_b, respectively, the normal flux density μH_n is continuous. If there is no surface current density, the tangential components H_t are also continuous. Thus, the magnetic field intensity to either side of the interface is as shown in Fig. 9.6.3. With the angles between **H** and the normal on each side of the interface denoted by α and β, respectively,

$$\tan \alpha = \frac{H_t^a}{H_n^a}; \qquad \tan \beta = \frac{H_t^b}{H_n^b} \tag{29}$$

The continuity conditions can be used to express $\tan(\alpha)$ in terms of the fields on the (b) side of the interface, so it follows that

$$\frac{\tan \alpha}{\tan \beta} = \frac{\mu_a}{\mu_b} \tag{30}$$

In the limit where $\mu_a/\mu_b \to 0$, there are therefore two possibilities. Either $\tan(\alpha) \to 0$, so that $\alpha \to 0$ and **H** in region (a) becomes perpendicular to the boundary, or $\tan(\beta) \to \infty$ so that $\beta \to 90$ degrees and **H** in region (b) becomes tangential to the boundary. Which of these two possibilities pertains depends on the excitation configuration.

Excitation in Region of High Permeability.   In these configurations, a closed contour can be found within the highly permeable material that encircles current-carrying wires. For the coil at the center of the highly permeable sphere considered in Example 9.6.2, such a contour is as shown in Fig. 9.6.4. As $\mu_b \to \infty$, the flux density **B** also goes to infinity. In this limit, the flux escaping from the body can be ignored compared to that guided by the body. The boundary is therefore one at which the interior flux density is essentially tangential.
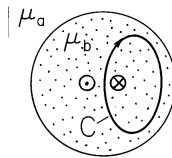
$$\mathbf{n} \cdot \mathbf{B} = 0 \tag{31}$$

Fig. 9.6.4   Typical contour in configuration of Fig. 9.6.1 encircling current without leaving highly permeable material.

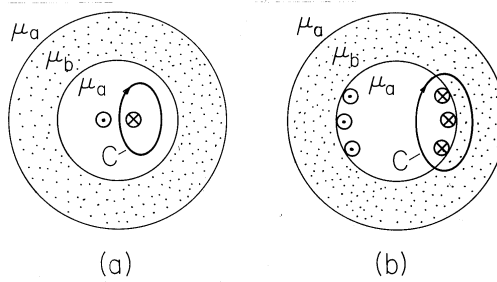(a)   (b)

Fig. 9.6.5   (a) With coil in the low permeability region, the contour encircling the current must pass through low permeability material. (b) With coil on the surface between regions, contours encircling current must still leave highly permeable region.

Once the field has been determined in the infinitely permeable material, continuity of tangential **H** is used to provide a boundary condition on the free space side of the interface.

Excitation in Region of Low Permeability.   In this second class of configurations, there is no closed contour within the highly permeable material that encircles a current-carrying wire. If the current-carrying wires are within the free space region, as in Fig. 9.6.5a, a contour must leave the highly permeable material to encircle the wire. In the limit where $\mu_b \to \infty$, the magnetic field intensity in the highly permeable material approaches zero, and thus **H** on the interior side of the interface becomes perpendicular to the boundary.

$$\mathbf{n} \times \mathbf{H} = 0 \qquad (32)$$

With wires on the interface between regions comprising a surface current density, as illustrated in Fig. 9.6.5b, it is still not possible to encircle the current without following a contour that leaves the highly permeable material. Thus, the case of a surface current is also in this second category. The tangential **H** is terminated by the surface current density. Thus, the boundary condition on **H** on the interior side of the interface carrying the surface current **K** is

$$\mathbf{n} \times \mathbf{H} = \mathbf{K} \qquad (33)$$

This boundary condition was illustrated in Example 9.6.1.

Once the fields in the interior region have been found, continuity of normal flux density provides a boundary condition for determining the flux distribution in the highly permeable region.
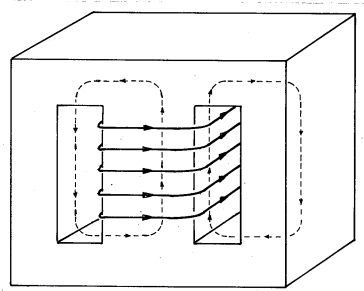
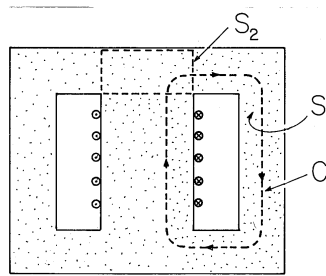**Fig. 9.7.1**   Highly magnetizable core in which flux induced by winding can circulate in two paths.

Fig. 9.7.2   Cross-section of highly permeable core showing contour C_1 spanned by surface S_1, used with Ampére's integral law, and closed surface S_2, used with the integral flux continuity law.

9.7 MAGNETIC CIRCUITS

The availability of relatively inexpensive magnetic materials, with magnetic susceptibilities of the order of 1000 or more, allows the production of high magnetic flux densities with relatively small currents. Devices designed to exploit these materials include compact inductors, transformers, and rotating machines. Many of these are modeled as the magnetic circuits that are the theme of this section.

A magnetic circuit typical of transformer cores is shown in Fig. 9.7.1. A core of high permeability material has a pair of rectangular windows cut through its center. Wires passing through these windows are wrapped around the central column. The flux generated by this coil tends to be guided by the magnetizable material. It passes upward through the center leg of the material, and splits into parts that circulate through the legs to left and right.

Example 9.6.2, with its highly permeable sphere excited by a small coil, offered the opportunity to study the trapping of magnetic flux. Here, as in that case with $\mu_b/\mu_a \gg 1$, the flux density inside the core tends to be tangential to the surface. Thus, the magnetic flux density is guided by the material and the field distribution within the core tends to be independent of the exterior configuration.

In situations of this type, where the ducting of the magnetic flux makes it possible to approximate the distribution of magnetic field, the MQS integral laws serve much the same purpose as do Kirchhoff's laws for electrical circuits.
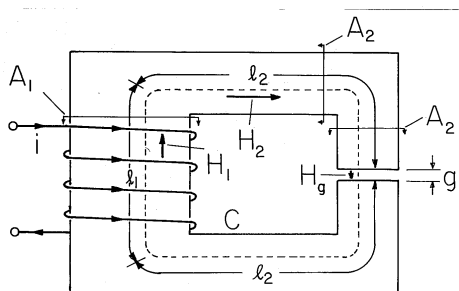
Fig. 9.7.3 Cross-section of magnetic circuit used to produce a magnetic field intensity H_g in an air gap.

The MQS form of Ampère's integral law applies to a contour, such as C_1 in Fig. 9.7.2, following a path of circulating magnetic flux.

$$\oint_{C_1} \mathbf{H} \cdot d\mathbf{s} = \int_{S_1} \mathbf{J} \cdot d\mathbf{a} \tag{1}$$

The surface enclosed by this contour in Fig. 9.7.2 is pierced N times by the current carried by the wire, so the surface integral of the current density on the right in (1) is, in this case, Ni. The same equation could be written for a contour circulating through the left leg, or for one circulating around through the outer legs. Note that the latter would enclose a surface S through which the net current would be zero.

If Ampère's integral law plays a role analogous to Kirchhoff's voltage law, then the integral law expressing continuity of magnetic flux is analogous to Kirchhoff's current law. It requires that through a closed surface, such as S_2 in Fig. 9.7.2, the net magnetic flux is zero.

$$\oint_{S_2} \mathbf{B} \cdot d\mathbf{a} = 0 \tag{2}$$

As a result, the flux entering the closed surface S_2 in Fig. 9.7.2 through the central leg must be equal to that leaving to left and right through the upper legs of the magnetic circuit. We will return to this particular magnetic circuit when we discuss transformers.

Example 9.7.1.   The Air Gap Field of an Electromagnet

The magnetic circuit of Fig. 9.7.3 might be used to produce a high magnetic field intensity in the narrow air gap. An N-turn coil is wrapped around the left leg of the highly permeable core. Provided that the length g of the air gap is not too large, the flux resulting from the current i in this winding is largely guided along the magnetizable material.

By approximating the fields in sections of the circuit as being essentially uniform, it is possible to use the integral laws to determine the field intensity in the gap. In the left leg, the field is approximated by the constant H_1 over the length l_1 and cross-sectional area A_1. Similarly, over the lengths l_2, which have the cross-sectional areas A_2, the field intensity is approximated by H_2. Finally, under the assumption that the gap width g is small compared to the cross-sectional dimensions of the gap, the field in the gap is represented by the constant H_g. The line

integral of $\mathbf{H}$ in Ampère's integral law, (1), is then applied to the contour C that follows the magnetic field intensity around the circuit to obtain the left-hand side of the expression

$$H_1 l_l + 2H_2 l_2 + g H_g = Ni \tag{3}$$

The right-hand side of this equation represents the surface integral of $\mathbf{J} \cdot \mathbf{da}$ for a surface S having this contour as its edge. The total current through the surface is simply the current through one wire multiplied by the number of times it pierces the surface S.

     We presume that the magnetizable material is operated under conditions of magnetic linearity. The constitutive law then relates the flux density and field intensity in each of the regions.

$$B_1 = \mu H_1; \quad B_2 = \mu H_2; \quad B_g = \mu_o H_g \tag{4}$$

Continuity of magnetic flux, (2), requires that the total flux through each section of the circuit be the same. With the flux densities expressed using (4), this requires that

$$A_1 \mu H_1 = A_2 \mu H_2 = A_2 \mu_o H_g \tag{5}$$

Our objective is to determine H_g. To that end, (5) is used to write

$$H_2 = \frac{\mu_o}{\mu} H_g; \qquad H_1 = \frac{\mu_o}{\mu} \frac{A_2}{A_1} H_g \tag{6}$$

and these relations used to eliminate H_1 and H_2 in favor of H_g in (3). From the resulting expression, it follows that

$$H_g = \frac{Ni}{\left(\frac{\mu_o}{\mu} \frac{A_2}{A_1} l_1 + \frac{2\mu_o}{\mu} l_2 + g \right)} \tag{7}$$

Note that in the limit of infinite core permeability, the gap field intensity is simply Ni/g.

     If the magnetic circuit can be broken into sections in which the field intensity is essentially uniform, then the fields may be determined from the integral laws. The previous example is a case in point. A more general approach is required if the core is of complex geometry or if a more accurate model is required.

     We presume throughout this chapter that the magnetizable material is sufficiently insulating so that even if the fields are time varying, there is no current density in the core. As a result, the magnetic field intensity in the core can be represented in terms of the scalar magnetic potential introduced in Sec. 8.3.

$$\mathbf{H} = -\nabla \Psi \tag{8}$$

     According to Ampère's integral law, (1), integration of $\mathbf{H} \cdot d\mathbf{s}$ around a closed contour must be equal to the "Ampère turns" Ni passing through the surface spanning the contour. With $\mathbf{H}$ expressed in terms of Ψ, integration from (a) to (b) around a contour such as C in Fig. 9.7.4, which encircles a net current equal to the product of the turns N and the current per turn i, gives $\Psi_a - \Psi_b \equiv \Delta \Psi = Ni$. With (a) and (b) adjacent to each other, it is clear that Ψ is multiple-valued. To specify the principal value of this multiple-valued function we must introduce a
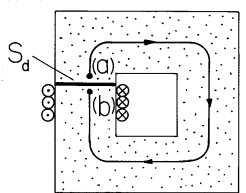
Fig. 9.7.4 Typical magnetic circuit configuration in which the magnetic scalar potential is first determined inside the highly magnetizable material. The principal value of the multivalued scalar potential inside the core is taken by not crossing the surface S_d.

discontinuity in Ψ somewhere along the contour. In the circuit of Fig. 9.7.4, this discontinuity is defined to occur across the surface S_d.

To make the line integral of $\mathbf{H} \cdot d\mathbf{s}$ from any point just above the surface S_d around the circuit to a point just below the surface equal to Ni, the potential is required to suffer a discontinuity $\Delta\Psi = Ni$ across S_d. Everywhere inside the magnetic material, Ψ satisfies Laplace's equation. If, in addition, the normal flux density on the walls of the magnetizable material is required to vanish, the distribution of Ψ within the core is uniquely determined. Note that only the discontinuity in Ψ is specified on the surface S_d. The magnitude of Ψ on one side or the other is not specified. Also, the normal derivative of Ψ, which is proportional to the normal component of $\mathbf{H}$, must be continuous across S_d.

The following simple example shows how the scalar magnetic potential can be used to determine the field inside a magnetic circuit.

Example 9.7.2.   The Magnetic Potential inside a Magnetizable Core

The core of the magnetic circuit shown in Fig. 9.7.5 has outer and inner radii a and b, respectively, and a length d in the z direction that is large compared to a. A current i is carried in the z direction through the center hole and returned on the outer periphery by N turns. Thus, the integral of $\mathbf{H} \cdot d\mathbf{s}$ over a contour circulating around the magnetic circuit must be Ni, and a surface of discontinuity S_d is arbitrarily introduced as shown in Fig. 9.7.5. With the boundary condition of no flux leakage, $\partial\Psi/\partial r = 0$ at $r = a$ and at $r = b$, the solution to Laplace's equation within the core is uniquely specified.

In principle, the boundary value problem can be solved even if the geometry is complicated. For the configuration shown in Fig. 9.7.5, the requirement of no radial derivative suggests that Ψ is independent of r. Thus, with A an arbitrary coefficient, a reasonable guess is

$$\Psi = A\phi = -Ni\left(\frac{\phi}{2\pi}\right) \tag{9}$$

The coefficient A has been selected so that there is indeed a discontinuity Ni in Ψ between $\phi = 2\pi$ and $\phi = 0$.

The magnetic field intensity given by substituting (9) into (8) is

$$\mathbf{H} = \frac{A}{r}\mathbf{i}_\phi = \frac{Ni}{2\pi r}\mathbf{i}_\phi \tag{10}$$

Note that $\mathbf{H}$ is continuous, as it should be.

Now that the inside field has been determined, it is possible, in turn, to find the fields in the surrounding free space regions. The solution for the inside field, together
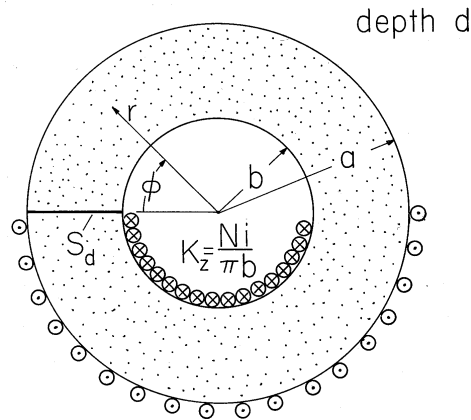
Fig. 9.7.5 Magnetic circuit consisting of a core having the shape of a circular cylindrical annulus with an N-turn winding wrapped around half of its circumferential length. The length of the system into the paper is very long compared to the outer radius a.

with the given surface current distribution at the boundary between regions, provides the tangential field at the boundaries of the outside regions. Within an arbitrary constant, a boundary condition on Ψ is therefore specified. In the outside regions, there is no closed contour that both stays within the region and encircles current. In these regions, Ψ is continuous. Thus, the problem of finding the "leakage" fields is reduced to finding the boundary value solution to Laplace's equation.

This inside-outside approach gives an approximate field distribution that is justified only if the relative permeability of the core is very large. Once the outside field is approximated in this way, it can be used to predict how much flux has left the magnetic circuit and hence how much error there is in the calculation. Generally, the error will be found to depend not only on the relative permeability but also on the geometry. If the magnetic circuit is composed of legs that are long and thin, then we would expect the leakage of flux to be large and the approximation of the inside-outside approach to become invalid.

Electrical Terminal Relations and Characteristics.   Practical inductors (chokes) often take the form of magnetic circuits. With more than one winding on the same magnetic circuit, the magnetic circuit serves as the core of a transformer. Figure 9.7.6 gives the schematic representation of a transformer. Each winding is modeled as perfectly conducting, so its terminal voltage is given by (9.2.12).

$$v_1 = \frac{d\lambda_1}{dt}; \qquad v_2 = \frac{d\lambda_2}{dt} \tag{11}$$

However, the flux linked by one winding is due to two currents. If the core is magnetically linear, we have a flux linked by the first coil that is the sum of a flux linkage $L_{11}i_1$ due to its own current and a flux linkage L_{12} due to the current in the second winding. The situation for the second coil is similar. Thus, the flux linkages are related to the terminal currents by an *inductance matrix*.

$$\begin{bmatrix} \lambda_1 \\ \lambda_2 \end{bmatrix} = \begin{bmatrix} L_{11} & L_{12} \\ L_{21} & L_{22} \end{bmatrix} \begin{bmatrix} i_1 \\ i_2 \end{bmatrix} \tag{12}$$
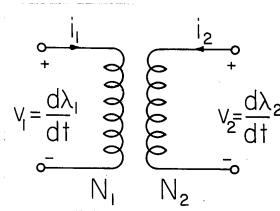
Fig. 9.7.6   Circuit representation of a transformer as defined by the terminal relations of (12) or of an ideal transformer as defined by (13).

The coefficients L_{ij} are functions of the core and coil geometries and properties of the material, with L_{11} and L_{22} the familiar *self-inductances* and L_{12} and L_{21} the *mutual inductances*.

The word "transformer" is commonly used in two ways, each often represented schematically, as in Fig. 9.7.6. In the first, the implication is only that the terminal relations are as summarized by (12). In the second usage, where the device is said to be an *ideal transformer*, the terminal relations are given as voltage and current ratios. For an ideal transformer,

$$\frac{i_2}{i_1} = -\frac{N_1}{N_2}; \qquad \frac{v_2}{v_1} = \frac{N_2}{N_1} \tag{13}$$

Presumably, such a device can serve to step up the voltage while stepping down the current. The relationships between terminal voltages and between terminal currents is linear, so that such a device is "ideal" for processing signals.

The magnetic circuit developed in the next example is that of a typical transformer. We have two objectives. First, we determine the inductances needed to complete (12). Second, we define the conditions under which such a transformer operates as an ideal transformer.

Example 9.7.3.   A Transformer

The core shown in Fig. 9.7.7 is familiar from the introduction to this section, Fig. 9.7.1. The "windows" have been filled up by a pair of windings, having the turns N_1 and N_2, respectively. They share the center leg of the magnetic circuit as a common core and generate a flux that circulates through the branches to either side.

The relation between the terminal voltages for an ideal transformer depends only on unity coupling between the two windings. That is, if we call Φ_λ the magnetic flux through the center leg, the flux linking the respective coils is

$$\lambda_1 = N_1 \Phi_\lambda; \qquad \lambda_2 = N_2 \Phi_\lambda \tag{14}$$

These statements presume that there is no leakage flux which would link one coil but bypass the other.

In terms of the magnetic flux through the center leg, the terminal voltages follow from (14) as

$$v_1 = N_1 \frac{d\Phi_\lambda}{dt}; \qquad v_2 = N_2 \frac{d\Phi_\lambda}{dt} \tag{15}$$

From these expressions, without further restrictions on the mode of operation, follows the relation between the terminal voltages of (13).
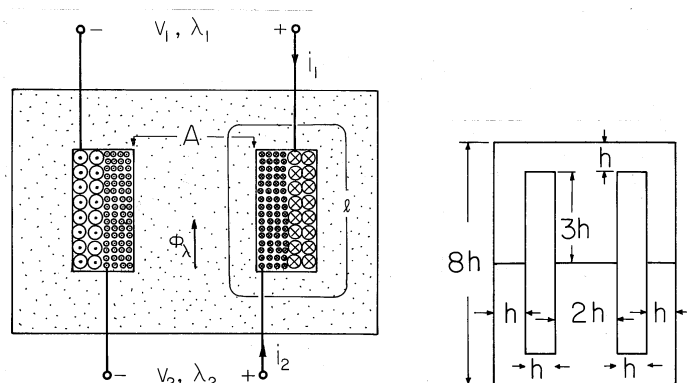
Fig. 9.7.7   In a typical transformer, coupling is optimized by wrapping
the primary and secondary on the same core. The inset shows how full
use is made of the magnetizable material in the core manufacture.

We now use the integral laws to determine the flux linkages in terms of the
currents. Because it is desirable to minimize the peak magnetic flux density at each
point throughout the core, and because the flux through the center leg divides evenly
between the two circuits, the cross-sectional areas of the return legs are made half
as large as that of the center leg.[3] As a result, the magnitude of **B**, and hence **H**,
can be approximated as constant throughout the core. [Note that we have now used
the flux continuity condition of (2).]

With the average length of a circulating magnetic field line taken as l, Ampère's
integral law, (1), gives

$$Hl = N_1 i_1 + N_2 i_2 \tag{16}$$

In view of the presumed magnetic linearity of the core, the flux through the cross-
sectional area A of the center leg is

$$\Phi_\lambda = AB = A\mu H \tag{17}$$

and it follows from these last two expressions that

$$\Phi_\lambda = \frac{A\mu N_1}{l} i_1 + \frac{A\mu N_2}{l} i_2. \tag{18}$$

Multiplication by the turns N_1 and then N_2, respectively, gives the flux linkages λ_1
and λ_2.

$$\lambda_1 = \left(\frac{A\mu N_1^2}{l} \right) i_1 + \left(\frac{A\mu N_1 N_2}{l} \right) i_2$$

$$\lambda_2 = \left(\frac{A\mu N_1 N_2}{l} \right) i_1 + \left(\frac{A\mu N_2^2}{l} \right) i_2 \tag{19}$$

---

[3] To optimize the usage of core material, the relative dimensions are often taken as in the
inset to Fig. 9.7.7. Two cores are cut from rectangular sections measuring $6h \times 8h$. Once the
windows have been removed, the rectangle is cut in two, forming two "E" cores which can then
be combined with the "I's" to form two complete cores. To reduce eddy currents, the core is often
made from varnished laminations. This will be discussed in Chap. 10.
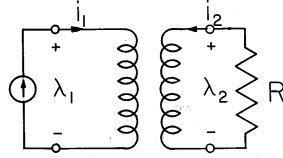
Fig. 9.7.8   Transformer with a load resistance R that includes the internal resistance of the secondary winding.

Comparison of this expression with (12) identifies the self- and mutual inductances as

$$L_{11} = \frac{A\mu N_1^2}{l}; \quad L_{22} = \frac{A\mu N_2^2}{l}; \quad L_{12} = L_{21} = \frac{A\mu N_1 N_2}{l} \tag{20}$$

Note that the mutual inductances are equal. In Sec. 11.7, we shall see that this is a consequence of energy conservation. Also, the self-inductances are related to either mutual inductance by

$$\sqrt{L_{11} L_{22}} = L_{12} \tag{21}$$

Under what conditions do the terminal currents obey the relations for an "ideal transformer"?

Suppose that the (1) terminals are selected as the "primary" terminals of the transformer and driven by a current source $I(t)$, and that the terminals of the (2) winding, the "secondary," are connected to a resistive load R. To recognize that the winding in fact has an internal resistance, this load includes the winding resistance as well. The electrical circuit is as shown in Fig. 9.7.8.

The secondary circuit equation is

$$-i_2 R = \frac{d\lambda_2}{dt} \tag{22}$$

and using (12) with $i_1 = I$, it follows that the secondary current i_2 is governed by

$$L_{22} \frac{di_2}{dt} + i_2 R = -L_{21} \frac{dI}{dt} \tag{23}$$

For purposes of illustration, consider the response to a drive that is in the sinusoidal steady state. With the drive angular frequency equal to ω, the response has the same time dependence in the steady state.

$$I = Re \; \hat{I} e^{j\omega t} \Rightarrow i_2 = Re \; \hat{i}_2 e^{j\omega t} \tag{24}$$

Substitution into (23) then shows that the complex amplitude of the response is

$$\hat{i}_2 = -\frac{j\omega L_{21} \hat{I}}{j\omega L_{22} + R} = -\frac{N_1}{N_2} \hat{i}_1 \frac{1}{1 + \frac{R}{j\omega L_{22}}} \tag{25}$$

The ideal transformer-current relation is obtained if

$$\frac{\omega L_{22}}{R} \gg 1 \tag{26}$$

In that case, (25) reduces to

$$\hat{i}_2 = -\frac{N_1}{N_2} \hat{i}_1 \tag{27}$$

When the ideal transformer condition, (26), holds, the first term on the left in (23) overwhelms the second. What remains if the resistance term is neglected is the statement

$$\frac{d}{dt}(L_{21}i_1 + L_{22}i_2) = \frac{d\lambda_2}{dt} = 0 \tag{28}$$

We conclude that *for ideal transformer operation, the flux linkages are negligible.* This is crucial to having a transformer behave as a linear device. Whether represented by the inductance matrix of (12) or by the ideal relations of (13), linear operation hinges on having a linear relation between **B** and **H** in the core, (17). By operating in the regime of (26) so that **B** is small enough to avoid saturation, (17) tends to remain valid.

9.8 SUMMARY

The magnetization density **M** represents the density of magnetic dipoles. The moment **m** of a single microscopic magnetic dipole was defined in Sec. 8.2. With $\mu_o\mathbf{m} \leftrightarrow \mathbf{p}$ where **p** is the moment of an electric dipole, the magnetic and electric dipoles play analogous roles, and so do the H and E fields. In Sec. 9.1, it was therefore natural to define the magnetization density so that it played a role analogous to the polarization density, $\mu_o\mathbf{M} \leftrightarrow \mathbf{P}$. As a result, the magnetic charge density ρ_m was considered to be a source of $\nabla \cdot \mu_o\mathbf{H}$. The relations of these sources to the magnetization density are the first expressions summarized in Table 9.8.1. The second set of relations are different forms of the flux continuity law, including the effect of magnetization. If the magnetization density is given, (9.2.2) and (9.2.3) are most useful. However, if **M** is induced by **H**, then it is convenient to introduce the magnetic flux density **B** as a variable. The correspondence between the fields due to magnetization and those due to polarization is $\mathbf{B} \leftrightarrow \mathbf{D}$.

The third set of relations pertains to linearly magnetizable materials. There is no magnetic analog to the unpaired electric charge density.

In this chapter, the MQS form of Ampère's law was also required to determine **H**.

$$\nabla \times \mathbf{H} = \mathbf{J} \tag{1}$$

In regions where **J**=0, **H** is indeed analogous to **E** in the polarized EQS systems of Chap. 6. In any case, if **J** is given, or if it is on perfectly conducting surfaces, its contribution to the magnetic field intensity is determined as in Chap. 8.

In Chap. 10, we introduce the additional laws required to determine **J** self-consistently in materials of finite conductivity. To do this, it is necessary to give careful attention to the electric field associated with MQS fields. In this chapter, we have generalized Faraday's law, (9.2.11),

$$\nabla \times \mathbf{E} = -\frac{\partial \mathbf{B}}{\partial t} \tag{2}$$

so that it can be used to determine **E** in the presence of magnetizable materials. Chapter 10 brings this law to the fore as it plays a key role in determining the self-consistent **J**.

TABLE 9.8.1 SUMMARY OF MAGNETIZATION RELATIONS AND LAWS			
Magnetization Charge Density and Magnetization Density			
$\rho_m \equiv -\nabla \cdot \mu_o \mathbf{M}$	(9.2.4)	$\sigma_{sm} = -\mathbf{n} \cdot \mu_o(\mathbf{M}^a - \mathbf{M}^b)$	(9.2.5)
Magnetic Flux Continuity with Magnetization			
$\nabla \cdot \mu_o \mathbf{H} = \rho_m$	(9.2.2)	$\mathbf{n} \cdot \mu_o(\mathbf{H}^a - \mathbf{H}^b) = \sigma_{sm}$	(9.2.3)
$\nabla \cdot \mathbf{B} = 0$	(9.2.9)	$\mathbf{n} \cdot (\mathbf{B}^a - \mathbf{B}^b) = 0$	(9.2.10)
where			
$\mathbf{B} \equiv \mu_o(\mathbf{H} + \mathbf{M})$	(9.2.8)		
Magnetically Linear Magnetization			
Constitutive law			
$\mathbf{M} = \chi_m \mathbf{H}; \chi_m \equiv \dfrac{\mu}{\mu_o} - 1$	(9.4.3)		
$\mathbf{B} = \mu \mathbf{H}$	(9.4.4)		
Magnetization source distribution			
$\rho_m = -\dfrac{\mu_o}{\mu} \mathbf{H} \cdot \nabla \mu$	(9.5.21)	$\sigma_{sm} = \mathbf{n} \cdot \mu_o \mathbf{H}^a \left(1 - \dfrac{\mu_a}{\mu_b}\right)$	(9.5.22)

R E F E R E N C E S

[1] Purcell, E. M., **Electricity and Magnetism**, McGraw-Hill Book Co., N. Y., 2nd Ed., (1985), p. 413.

P R O B L E M S

9.2 Laws and Continuity Conditions with Magnetization

9.2.1   Return to Prob. 6.1.1 and replace $\mathbf{P} \to \mathbf{M}$. Find ρ_m and σ_{sm}.

9.2.2*   A circular cylindrical rod of material is uniformly magnetized in the y' direction transverse to its axis, as shown in Fig. P9.2.2. Thus, for $r < R$, $\mathbf{M} = M_o[\mathbf{i_x} \sin \gamma + \mathbf{i_y} \cos \gamma]$. In the surrounding region, the material forces $\mathbf{H}$ to be zero. (In Sec. 9.6, it will be seen that such a material is one of infinite permeability.)
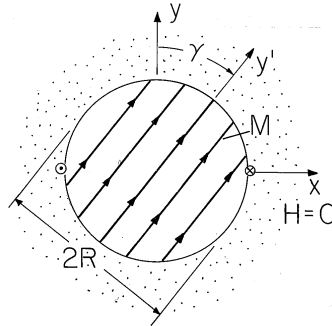
Fig. P9.2.2

(a) Show that if $\mathbf{H} = \mathbf{0}$ everywhere, both Ampère's law and (9.2.2) are satisfied.

(b) Suppose that the cylinder rotates with the angular velocity Ω so that $\gamma = \Omega t$. Then, $\mathbf{B}$ is time varying even though there is no $\mathbf{H}$. A one-turn rectangular coil having depth d in the z direction has legs running parallel to the z axis in the $+z$ direction at $x = -R$, $y = 0$ and in the $-z$ direction at $x = R$, $y = 0$. The other legs of the coil are perpendicular to the z axis. Show that the voltage induced at the terminals of this coil by the time-varying magnetization density is $v = -\mu_o 2RdM_o\Omega \sin \Omega t$.
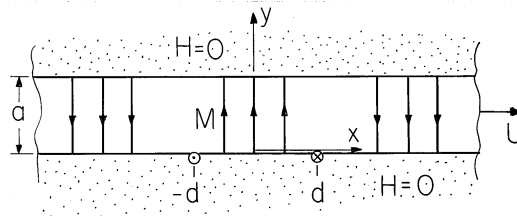
Fig. P9.2.3
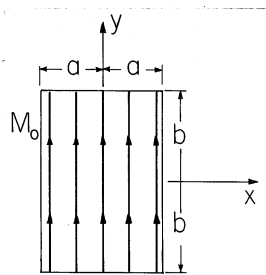
Fig. P9.3.1

9.2.3   In a region between the planes $y = a$ and $y = 0$, a material that moves
in the x direction with velocity U has the magnetization density $\mathbf{M} = M_o \mathbf{i_y} \cos \beta (x - Ut)$, as shown in Fig. P9.2.2. The regions above and below
are constrained so that $\mathbf{H} = \mathbf{0}$ there and so that the integral of $\mathbf{H} \cdot d\mathbf{s}$
between $y = 0$ and $y = a$ is zero. (In Sec. 9.7, it will be clear that these
materials could be the pole faces of a highly permeable magnetic circuit.)

   (a) Show that Ampère's law and (9.2.2) are satisfied if $\mathbf{H} = \mathbf{0}$ throughout
   the magnetizable layer of material.

   (b) A one-turn rectangular coil is located in the $y = 0$ plane, one leg
   running in the $+z$ direction at $x = -d$ (from $z = 0$ to $z = l$) and
   another running in the $-z$ direction at $x = d$ (from $z = l$ to $z = 0$).
   What is the voltage induced at the terminals of this coil by the motion
   of the layer?

9.3 Permanent Magnetization

9.3.1*   The magnet shown in Fig. P9.3.1 is much longer in the $\pm z$ directions than
either of its cross-sectional dimensions $2a$ and $2b$. Show that the scalar
magnetic potential is

$$
\Psi = \frac{M_o}{2\pi} \left\{ (x - a) ln \frac{\sqrt{(x-a)^2 + (y-b)^2}}{\sqrt{(x-a)^2 + (y+b)^2}} \right.
$$
$$
- (x + a) ln \frac{\sqrt{(x+a)^2 + (y-b)^2}}{\sqrt{(x+a)^2 + (y+b)^2}}
$$
$$
+ (y - b) \left[\tan^{-1} \left(\frac{x-a}{y-b} \right) - \tan^{-1} \left(\frac{x+a}{y-b} \right) \right]
$$
$$
\left. - (y + b) \left[\tan^{-1} \left(\frac{x-a}{y+b} \right) - \tan^{-1} \left(\frac{x+a}{y+b} \right) \right] \right\}
\qquad (a)
$$

(Note Example 4.5.3.)

9.3.2[*] In the half-space $y > 0$, $\mathbf{M} = M_o \cos(\beta x) \exp(-\alpha y)\mathbf{i_y}$, where α and β are given positive constants. The half-space $y < 0$ is free space. Show that

$$\Psi = \frac{M_o}{2} \begin{cases} \left[\frac{-2\alpha}{\alpha^2 - \beta^2} e^{-\alpha y} + \frac{e^{-\beta y}}{\alpha - \beta} \right] \cos \beta x; & y > 0 \\ -\frac{e^{\beta y}}{\alpha + \beta} \cos \beta x; & y < 0 \end{cases} \qquad (a)$$

9.3.3 In the half-space $y < 0$, $\mathbf{M} = M_o \sin(\beta x) \exp(\alpha y)\mathbf{i_x}$, where α and β are positive constants. The half-space $y > 0$ is free space. Find the scalar magnetic potential.
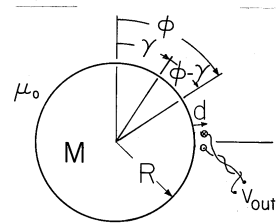
Fig. P9.3.4

9.3.4 For storage of information, the cylinder shown in Fig. P9.3.4 has the magnetization density

$$\mathbf{M} = M_o (r/R)^{p-1} [\mathbf{i_r} \cos p(\phi - \gamma) - \mathbf{i_\phi} \sin p(\phi - \gamma)] \qquad (a)$$

where p is a given integer. The surrounding region is free space.

(a) Determine the magnetic potential Ψ.
(b) A magnetic pickup is comprised of an N-turn coil located at $\phi = \pi/2$. This coil has a dimension a in the ϕ direction that is small compared to the periodicity length $2\pi R/p$ in that direction. Every turn is essentially at the radius $d + R$. Determine the output voltage v_{out} when the cylinder rotates, $\gamma = \Omega t$.
(c) Show that if the density of information on the cylinder is to be high (p is to be high), then the spacing between the coil and the cylinder, d, must be small.

9.4 Magnetization Constitutive Laws

9.4.1[*] The toroidal core of Example 9.4.1 and Demonstration 9.4.1 is filled by a material having the single-valued magnetization characteristic $\mathbf{M} = M_o$ tanh (αH), where $\mathbf{M}$ and $\mathbf{H}$ are collinear.

(a) Show that the $B - H$ characteristic is of the type illustrated in Fig. 9.4.4.
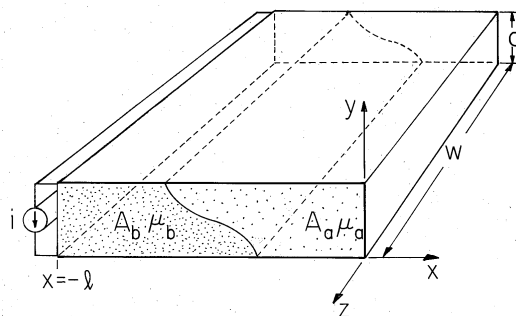
Fig. P9.5.1

(b) Show that if $i = i_o \cos \omega t$, the output voltage is

$$v = \frac{\mu_o \pi w^2 N_2}{4} \frac{d}{dt} \left[\frac{N_1 i_o}{2\pi R} \cos \omega t + M_o \tanh \left(\frac{\alpha N_1 i_o}{2\pi R} \cos \omega t \right) \right] \qquad (a)$$

(c) Show that the characteristic is essentially linear, provided that $\alpha N_1 i_o / 2\pi R \ll 1$.

9.4.2   The toroidal core of Demonstration 9.4.1 is driven by a sinusoidal current $i(t)$ and responds with the hysteresis characteristic of Fig. 9.4.6. Make qualitative sketches of the time dependence of

(a) $B(t)$
(b) the output voltage $v(t)$.

9.5 Fields in the Presence of Magnetically Linear Insulating Materials

9.5.1* A perfectly conducting sheet is bent into a $\supset$ shape to make a one-turn inductor, as shown in Fig. P9.5.1. The width w is much larger than the dimensions in the $x - y$ plane. The region inside the inductor is filled with two linearly magnetizable materials having permeabilities μ_a and μ_b, respectively. The cross-section of the system in any $x - y$ plane is the same. The cross-sectional areas of the magnetizable materials are A_a and A_b, respectively. Given that the current $i(t)$ is uniformly distributed over the width w of the inductor, show that $\mathbf{H} = (i/w)\mathbf{i_z}$ in both of the magnetizable materials. Show that the inductance $L = (\mu_a A_a + \mu_b A_b)/w$.

9.5.2   Perfectly conducting coaxial cylinders, shorted at one end, form the one-turn inductor shown in Fig. P9.5.2. The total current i flowing on the surface at $r = b$ of the inner cylinder is returned through the short and the outer conductor at $r = a$. The annulus is filled by materials of uniform permeability with an interface at $r = R$, as shown.

(a) Determine $\mathbf{H}$ in the annulus. (A simple solution can be shown to satisfy all the laws and continuity conditions.)
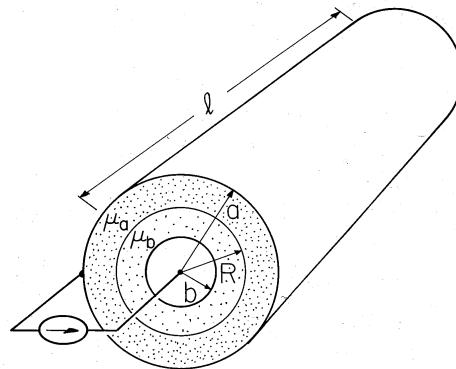
Fig. P9.5.2

(b) Find the inductance.

9.5.3* The piece-wise uniform material in the one-turn inductor of Fig. P9.5.1 is replaced by a smoothly inhomogeneous material having the permeability $\mu = -\mu_m x/l$, where μ_m is a given constant. Show that the inductance is $L = d\mu_m l/2w$.

9.5.4 The piece-wise uniform material in the one-turn inductor of Fig. P9.5.2 is replaced by one having the permeability $\mu = \mu_m(r/b)$, where μ_m is a given constant. Determine the inductance.

9.5.5* Perfectly conducting coaxial cylinders, shorted at one end, form a one-turn inductor as shown in Fig. P9.5.5. Current flowing on the surface at $r = b$ of the inner cylinder is returned on the inner surface of the outer cylinder at $r = a$. The annulus is filled by sectors of linearly magnetizable material, as shown.

   (a) Assume that in the regions (a) and (b), respectively, $\mathbf{H} = \mathbf{i}_\phi A/r$ and $\mathbf{H} = \mathbf{i}_\phi C/r$, and show that with A and C functions of time, these fields satisfy Ampère's law and the flux continuity law in the respective regions.
   (b) Use the flux continuity condition at the interfaces between regions to show that $C = (\mu_a/\mu_b)A$.
   (c) Use Ampère's integral law to relate C and A to the total current i in the inner conductor.
   (d) Show that the inductance is $L = l\mu_a \ln(a/b)/[\alpha + (2\pi - \alpha)\mu_a/\mu_b]$.
   (e) Show that the surface current densities at $r = b$ adjacent to regions (a) and (b), respectively, are $K_z = A/b$ and $K_z = C/b$.

9.5.6 In the one-turn inductor of Fig. P9.5.1, the material of piece-wise uniform permeability is replaced by another such material. Now the region between the plates in the range $0 < z < a$ is filled by material having uniform permeability μ_a, while $\mu = \mu_b$ in the range $a < z < w$. Determine the inductance.
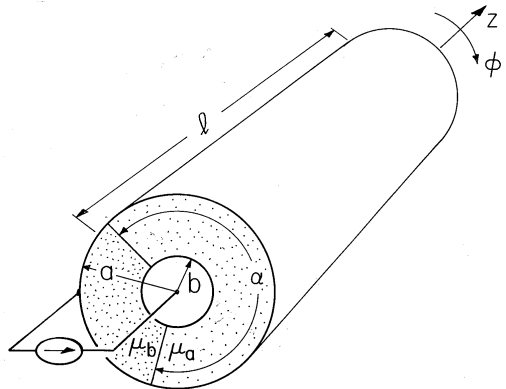
Fig. P9.5.5

9.6 Fields in Piece-Wise Uniform Magnetically Linear Materials

9.6.1[*]   A winding in the $y = 0$ plane is used to produce the surface current density $\mathbf{K} = K_o \cos \beta z \mathbf{i_x}$. Region (a), where $y > 0$, is free space, while region (b), where $y < 0$, has permeability μ.

(a) Show that

$$\Psi = \frac{K_o \sin \beta z}{\beta(1 + \mu/\mu_o)} \begin{cases} -\frac{\mu}{\mu_o} e^{-\beta y}; & y > 0 \\ e^{\beta y}; & y < 0 \end{cases} \tag{a}$$

(b) Now consider the same problem, but assume at the outset that the material in region (b) has infinite permeability. Show that it agrees with the limit $\mu \to \infty$ of the first expression of part (a).

(c) In turn, use the result of part (b) as a starting point in finding an approximation to Ψ in the highly permeable material. Show that this result agrees with the limit of the second result of part (a) where $\mu \gg \mu_o$.

9.6.2   The planar region $-d < y < d$ is bounded from above and below by infinitely permeable materials, as shown in Fig. P9.6.2. Region (a) to the right and region (b) to the left are separated by a current sheet in the plane $x = 0$ with the distribution $\mathbf{K} = \mathbf{i_z} K_o \sin(\pi y/2d)$. The system extends to infinity in the $\pm x$ directions and is two dimensional.

(a) In terms of Ψ, what are the boundary conditions at $y = \pm d$.

(b) What continuity conditions relate Ψ in regions (a) and (b) where they meet at $x = 0$?

(c) Determine Ψ.

9.6.3[*]   The cross-section of a two-dimensional cylindrical system is shown in Fig. P9.6.3. A region of free space having radius R is surrounded by material
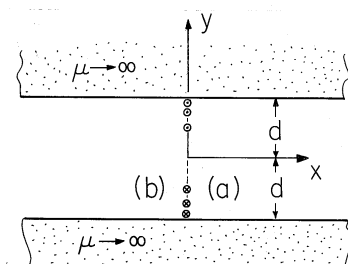
Fig. P9.6.2
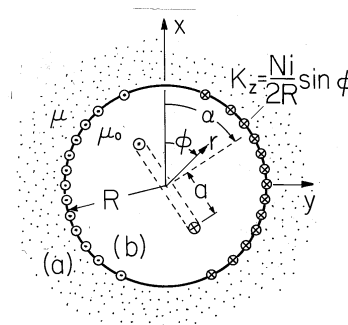
Fig. P9.6.3

having permeability μ which can be considered as extending to infinity. A winding at $r = R$ is driven by the current i and has turns density $(N/2R)\sin\phi$ (turns per unit length in the ϕ direction). Thus, at $r = R$, there is a current density $\mathbf{K} = (N/2R)i\sin\phi\mathbf{i_z}$.

(a) Show that

$$\Psi = \frac{(N/2)i\cos\phi}{(1 + \mu/\mu_o)} \left\{ \begin{array}{ll} \frac{R}{r}; & r > R \\ -(\mu/\mu_o)(r/R); & r < R \end{array} \right. \tag{a}$$

(b) An n-turn coil having a spacing between conductors of $2a$ is now placed at the center. The magnetic axis of this coil is inclined at the angle α relative to the x axis. This coil has length l in the z direction. Show that the mutual inductance between this coil and the one at $r = R$ is $L_m = \mu_o a \, ln N \cos\alpha/R[1 + (\mu_o/\mu)]$.

9.6.4 The cross-section of a motor or generator is shown in Fig. 11.7.7. The two coils comprising the stator and rotor windings and giving rise to the surface current densities of (11.7.24) and (11.7.25) have flux linkages having the forms given by (11.7.26).

(a) Assume that the permeabilities of the rotor and stator are infinite, and determine the vector potential in the air gap.
(b) Determine the self-inductances L_s and L_r and magnitude of the peak mutual inductance, M, in (11.7.26). Assume that the current in the $+z$ direction at ϕ is returned at $\phi + \pi$.
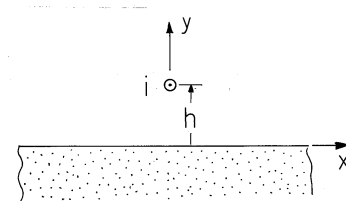
Fig. P9.6.5

9.6.5   A wire carrying a current i in the z direction is suspended a height h above the surface of a magnetizable material, as shown in Fig. P9.6.5. The wire extends to "infinity" in the $\pm z$ directions. Region (a), where $y > 0$, is free space. In region (b), where $y < 0$, the material has uniform permeability μ.

   (a) Use the method of images to determine the fields in the two regions.
   (b) Now assume that $\mu \gg \mu_o$ and find **H** in the upper region, assuming at the outset that $\mu \to \infty$.
   (c) In turn, use this approximate result to find the field in the permeable material.
   (d) Show that the results of (b) and (c) are consistent with those from the exact analysis in the limit where $\mu \gg \mu_o$.

9.6.6*   A conductor carries the current $i(t)$ at a height h above the upper surface of a material, as shown in Fig. P9.6.5. The force per unit length on the conductor is $\mathbf{f} = \mathbf{i} \times \mu_o\mathbf{H}$, where **i** is a vector having the direction and magnitude of the current $i(t)$, and **H** does not include the self-field of the line current.

   (a) Show that if the material is a perfect conductor, $\mathbf{f} = \mu_o\mathbf{i_y}i^2/4\pi h$.
   (b) Show that if the material is infinitely permeable, $\mathbf{f} = -\mu_o\mathbf{i_y}i^2/4\pi h$.

9.6.7*   Material having uniform permeability μ is bounded from above and below by regions of infinite permeability, as shown in Fig. P9.6.7. With its center at the origin and on the surface of the lower infinitely permeable material is a hemispherical cavity of free space having radius a that is much less than d. A field that has the uniform intensity H_o far from the hemispherical surface is imposed in the z direction.

   (a) Assume $\mu \gg \mu_o$ and show that the approximate magnetic potential in the magnetizable material is $\Psi = -H_o a[(r/a) + (a/r)^2/2]\cos\theta$.
   (b) In turn, show that the approximate magnetic potential inside the hemisphere is $\Psi = -3H_o z/2$.

9.6.8   In the magnetic tape configuration of Example 9.3.2, the system is as shown in Fig. 9.3.2 except that just below the tape, in the plane $y = -d/2$, there is an infinitely permeable material, and in the plane $y = a > d/2$ above the tape, there is a second infinitely permeable material. Find the voltage v_o.
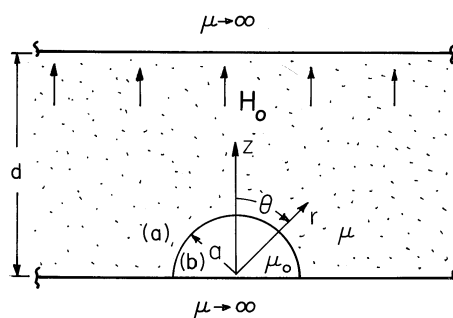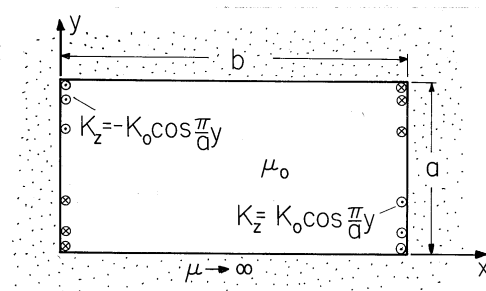
Fig. P9.6.7

Fig. P9.6.9

9.6.9[*]   A cylindrical region of free space of rectangular cross-section is surrounded by infinitely permeable material, as shown in Fig. P9.6.9. Surface currents are imposed by means of windings in the planes $x = 0$ and $x = b$. Show that

$$\Psi = \frac{K_o a}{\pi} \sin \frac{\pi y}{a} \frac{\cosh \frac{\pi}{a}\left(x - \frac{b}{2}\right)}{\cosh \left(\frac{\pi b}{2a}\right)} \tag{a}$$

9.6.10[*] A circular cylindrical hole having radius R is cut through a material having permeability μ_a. A conductor passing through this hole has permeability μ_b and carries the uniform current density $\mathbf{J} = J_o \mathbf{i_z}$, as shown in Fig. P9.6.10. A field that is uniform far from the hole, where it is given by $\mathbf{H} = H_o \mathbf{i_x}$, is applied by external means. Show that for $r < R$, and $R < r$, respectively,

$$A_z = \begin{cases} \frac{-\mu_b J_o r^2}{4} - \frac{2\mu_b H_o R}{(1+\mu_b/\mu_a)} \frac{r}{R} \sin\phi \\ \frac{-\mu_a J_o R^2}{2}\left[ln(r/R) + \frac{1}{2}\frac{\mu_b}{\mu_a}\right] - \mu_a H_o R\left[\frac{r}{R} - \frac{(\mu_a-\mu_b)}{(\mu_a+\mu_b)}\frac{R}{r}\right]\sin\phi \end{cases} \tag{a}$$

9.6.11[*] Although the introduction of a magnetizable sphere into a uniform magnetic field results in a distortion of that field, nevertheless, the field within the sphere is uniform. This fact makes it possible to determine the field distribution in and around a spherical particle even when its magnetization characteristic is nonlinear. For example, consider the fields in and around the sphere of material shown together with its $B - H$ curve in Fig. P9.6.11.
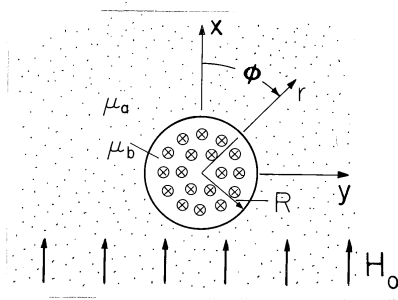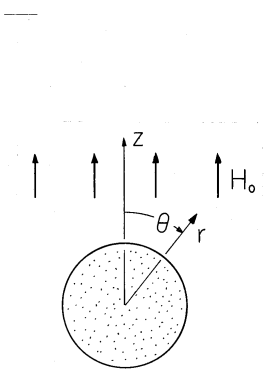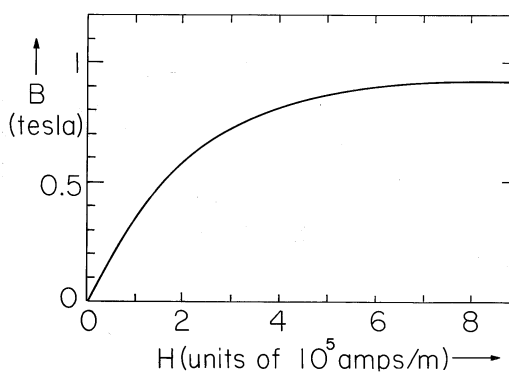
Fig. P9.6.10

Fig. P9.6.11

(a) Assume that the magnetization density is $\mathbf{M} = M\mathbf{i_z}$, where M is a constant to be determined, and show that the magnetic field intensity inside the sphere is uniform, z directed, and of magnitude $H = H_o - M/3$, and hence that the magnetic flux density, B, in the sphere is related to the magnitude of the magnetic field intensity H by

$$B = 3\mu_o H_o - 2\mu_o H \qquad (a)$$

(b) Draw this *load line* in the $B-H$ plane, showing that it is a straight line with intercepts $3H_o/2$ and $3\mu_o H_o$ with the H and B axes, respectively.

(c) Show how (B, H) in the sphere are determined, given the applied field intensity H_o, by graphically finding the point of intersection between the $B - H$ curve of Fig. P9.6.11 and (a).

(d) Show that if $H_o = 4 \times 10^5$ A/m, $B = 0.75$ tesla and $H = 3.1 \times 10^5$ A/m.

9.6.12 The circular cylinder of magnetizable material shown in Fig. P9.6.12 has the $B - H$ curve shown in Fig. P9.6.11. Determine $\mathbf{B}$ and $\mathbf{H}$ inside the cylinder resulting from the application of a field intensity $\mathbf{H} = H_o\mathbf{i_x}$ where $H_o = 4 \times 10^5$ A/m.
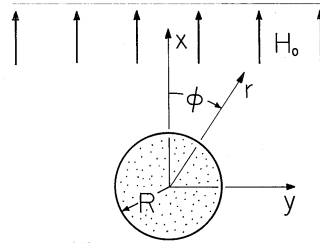
Fig. P9.6.12

9.6.13 The spherical coil of Example 9.6.1 is wound around a sphere of material having the $B - H$ curve shown in Fig. P9.6.11. Assume that $i = 800$ A, $N = 100$ turns, and $R = 10$ cm, and determine B and H in the material.

9.7 Magnetic Circuits

9.7.1* The magnetizable core shown in Fig. P9.7.1 extends a distance d into the paper that is large compared to the radius a. The driving coil, having N turns, has an extent Δ in the ϕ direction that is small compared to dimensions of interest. Assume that the core has a permeability μ that is very large compared to μ_o.

(a) Show that the approximate **H** and Ψ inside the core (with Ψ defined to be zero at $\phi = \pi$) are

$$\mathbf{H} = \frac{Ni}{2\pi r}\mathbf{i}_\phi; \qquad \Psi = \frac{Ni}{2}\Big(1 - \frac{\phi}{\pi}\Big) \tag{a}$$

(b) Show that the approximate magnetic potential in the central region is

$$\Psi = \sum_{m=1}^{\infty} \frac{Ni}{m\pi}(r/b)^m \sin m\phi \tag{b}$$

9.7.2 For the configuration of Prob. 9.7.1, determine Ψ in the region outside the core, $r > a$.

9.7.3* In the magnetic circuit shown in Fig. P9.7.3, an N-turn coil is wrapped around the center leg of an infinitely permeable core. The sections to right and left have uniform permeabilities μ_a and μ_b, respectively, and the gap lengths a and b are small compared to the other dimensions of these sections. Show that the inductance $L = N^2 w[(\mu_b d/b) + (\mu_a c/a)]$.

9.7.4 The magnetic circuit shown in Fig. P9.7.4 is constructed from infinitely permeable material, as is the hemispherical bump of radius R located on the surface of the lower pole face. A coil, having N turns, is wound around
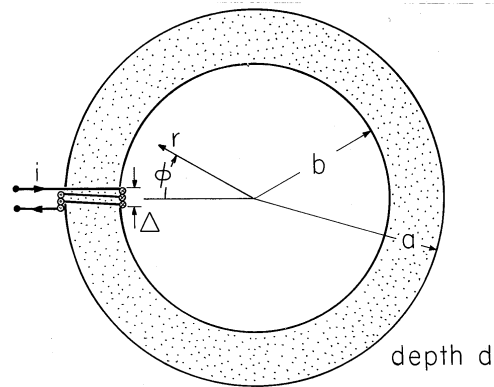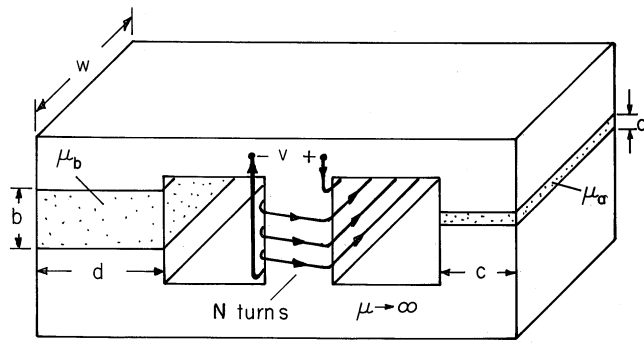
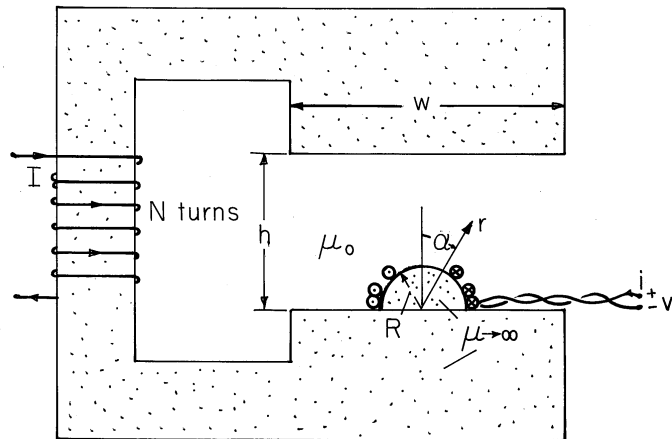**Fig. P9.7.1**

Fig. P9.7.3

depth w
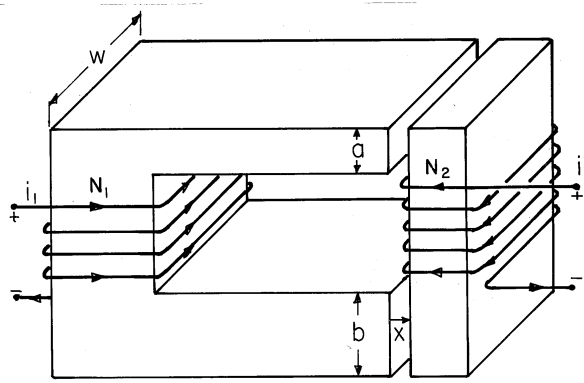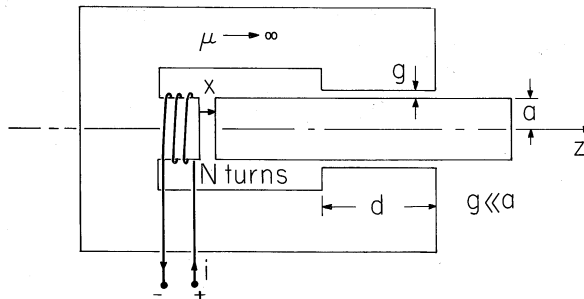

Fig. P9.7.4

Fig. P9.7.5

Fig. P9.7.6

the left leg of the magnetic circuit. A second coil is wound around the hemisphere in a distributed fashion. The turns per unit length, measured along the periphery of the hemisphere, is $(n/R)\sin\alpha$, where n is the total number of turns. Given that $R \ll h \ll w$, find the mutual inductance of the two coils.

9.7.5* The materials comprising the magnetic circuit of Fig. P9.7.5 can be regarded as having infinite permeability. The air gaps have a length x that is much less than a or b, and these dimensions, in turn, are much less than w. The coils to left and right, respectively, have total turns N_1 and N_2. Show that the self- and mutual inductances of the coils are

$$L_{11} = N_1^2 L_o, \quad L_{12} = L_{21} = N_1 N_2 L_o,$$

$$L_{22} = N_2^2 L_o, \quad L_o \equiv \frac{aw\mu_o}{x(1 + a/b)} \tag{a}$$

9.7.6 The magnetic circuit shown in Fig. P9.7.6 has rotational symmetry about the z axis. Both the circular cylindrical plunger and the remainder of the magnetic circuit can be regarded as infinitely permeable. The air gaps have
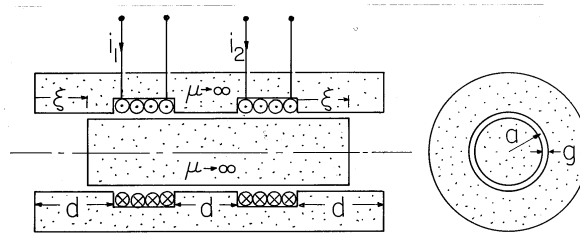
Fig. P9.7.7

widths x and g that are small compared to a and d. Determine the inductance of the coil.

9.7.7   Two cross-sectional views of an axisymmetric magnetic circuit that could be used as an electromechanical transducer are shown in Fig. P9.7.7. Surrounding an infinitely permeable circular cylindrical rod having a radius slightly less than a is an infinitely permeable stator having a hole down its center with a radius slightly greater than a. A pair of coils, having turns N_1 and N_2 and driven by currents i_1 and i_2, respectively are wound around the center rod and positioned in slots in the surrounding stator. The longitudinal position of the rod, denoted by ξ, is limited in range so that the ends of the rod are always well inside the ends of the stator. Thus, **H** in each of the air gaps is essentially uniform. Determine the inductance matrix, (9.7.12).

9.7.8   Fields in and around the magnetic circuit shown in Fig. P9.7.8 are to be considered as independent of z. The outside walls are infinitely permeable, while the horizontal central leg has uniform permeability μ that is much less than that of the sides but nevertheless much greater than μ_o. Coils having total turns N_1 and N_2, respectively, are wound around the center leg. These have evenly distributed turns in the planes $x = l/2$ and $x = -l/2$, respectively. The regions above and below the center leg are free space.

   (a) Define $\Psi = 0$ at the origin of the given coordinates. As far as Ψ is concerned inside the center leg, what boundary conditions must Ψ satisfy if the central leg is treated as the "inside" of an "inside-outside" problem?
   (b) What is Ψ in the center leg?
   (c) What boundary conditions must Ψ satisfy in region (a)?
   (d) What is Ψ, and hence **H**, in region (a)? (A simple exact solution is suggested by Prob. 7.5.3.) For the case where $N_1 i_1 = N_2 i_2$, sketch ψ and **H** in regions (a) and (b).

9.7.9   The magnetic circuit shown in Fig. P9.7.9 is excited by an N-turn coil and consists of infinitely permeable legs in series with ones of permeability μ, one to the right of length l_2 and the other to the left of length l_1. This second leg has wrapped on its periphery a metal strap having thickness $\Delta \ll w$, conductivity σ, and height l_1. With a terminal current $i = i_o \cos \omega t$, determine **H** within the left leg.
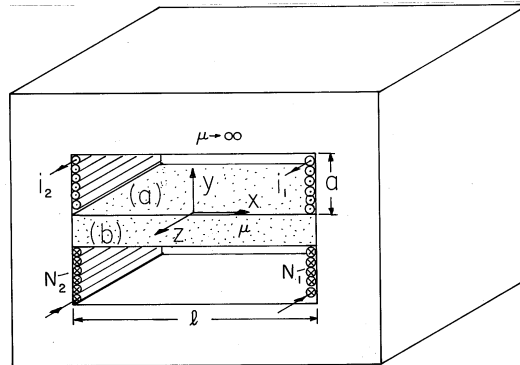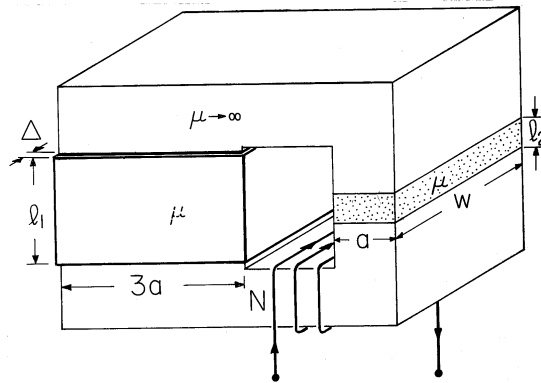
Fig. P9.7.8

Fig. P9.7.9

9.7.10* The graphical approach to determining fields in magnetic circuits to be used in this and the next example is similar to that illustrated by Probs. 9.6.11–9.6.13. The magnetic circuit of a high-field magnet is shown in Fig. P9.7.10. The two coils each have N turns and carry a current i.

   (a) Show that the *load line* for the circuit is

$$B = -\frac{\mu_o}{d}(l_2 + l_1)H + \frac{2Ni\mu_o}{d} \qquad (a)$$

   (b) For $N = 500$, $d = 1$ cm, $l_1 = 0.8m$, $l_2 = 0.2$ m, and $i = 10$ amps, find the flux density B in its air gap.

9.7.11 In the magnetic circuit of Fig. P9.7.11, the infinitely permeable core has a gap with cross-sectional area A and height $a + b$, where the latter is much less than the dimensions of the former. In this gap is a material having height b and the $M - H$ relation also shown in the figure. Within the material and in the air gap, $\mathbf{H}$ is approximated as being uniform.
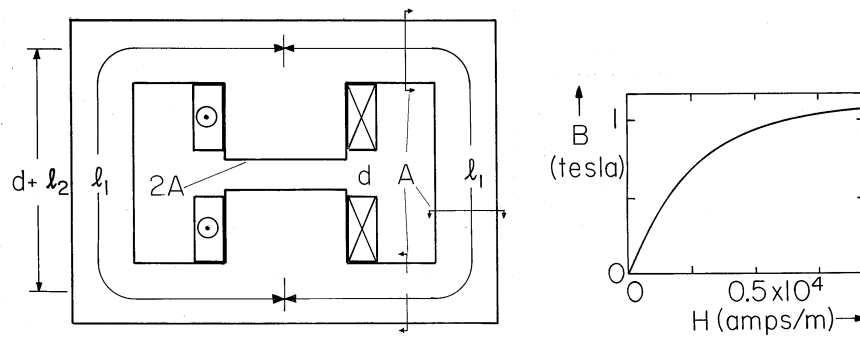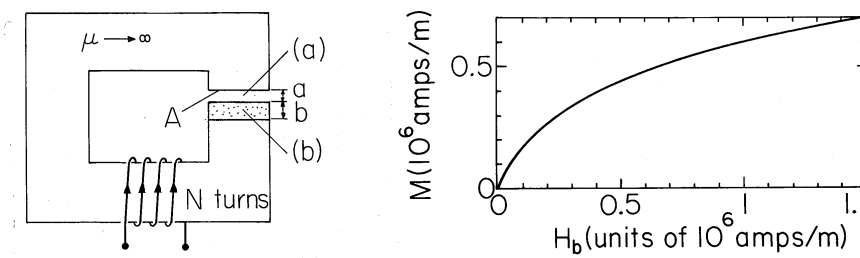
Fig. P9.7.10

Fig. P9.7.11

(a) Determine the load line relation between H_b, the field intensity in the material, M, and the driving current i.

(b) If $Ni/a = 0.5 \times 10^6$ amps/m and $b/a = 1$, what is M, and hence B?